EUROPEAN RESPIRATORY *journal*

FLAGSHIP SCIENTIFIC JOURNAL OF ERS

Early View

Original research article

Gut microbiota mediate vascular dysfunction in a murine model of sleep apnea: effect of probiotics

Mohammad Badran, Abdelnaby Khalyfa, Aaron Ericsson, Clementine Puech, Zachary McAdams, Shawn B Bender, David Gozal

Please cite this article as: Badran M, Khalyfa A, Ericsson A, *et al*. Gut microbiota mediate vascular dysfunction in a murine model of sleep apnea: effect of probiotics. *Eur Respir J* 2022; in press (https://doi.org/10.1183/13993003.00002-2022).

Gut microbiota mediate vascular dysfunction in a murine model of sleep apnea: effect of probiotics

Mohammad Badran[1], Abdelnaby Khalyfa[1], Aaron Ericsson[2,3], Clementine Puech[1], Zachary McAdams[4], Shawn B Bender[5,6,7], David Gozal*[1,8]

[1] Department of Child Health and Child Health Research Institute, School of Medicine, University of Missouri, Columbia, MO, United States

[2] Department of Veterinary Pathobiology, University of Missouri, Columbia, MO, United States

[3] University of Missouri Metagenomics Center, University of Missouri, Columbia, MO, United States

[4] Department of Molecular Microbiology and Immunology, Molecular Pathogeneses and Therapeutics Program University of Missouri, Columbia, MO, United States

[5] Dalton Cardiovascular Research Center, University of Missouri, Columbia, MO, United States

[6] Department of Biomedical Sciences, University of Missouri, Columbia, MO, United States

[7] Harry S. Truman Memorial Veterans Hospital, University of Missouri, Columbia, MO, United States

[8] Department of Medical Pharmacology and Physiology, School of Medicine, University of Missouri, Columbia, MO, United States

***Corresponding author:**

David Gozal, MD, MBA, PhD (Hon), ATSF
Department of Child Health and Child Health University of Missouri School of Medicine
400 N Keene St, Suite 010, Columbia, MO 65201, USA
Office: 573-882-6882
Fax: 573-884-5179
Email: gozald@health.missouri.edu

Take home summary: intermittent hypoxia-induced gut microbiome alterations elicit cardiovascular disturbances such as hypertension and coronary artery dysfunction that are prevented by probiotics administration

Abstract

Rationale: Obstructive sleep apnea (OSA) is a chronic prevalent condition characterized by intermittent hypoxia (IH) and is associated with endothelial dysfunction and coronary artery disease (CAD). OSA can induce major changes in gut microbiome (GM) diversity and composition, which in turn may induce the emergence of OSA-associated morbidities. However, the causal effects of IH-induced GM changes on the vasculature remain unexplored.

Objectives: To assess if vascular dysfunction induced by IH is mediated through GM changes.

Methods: Fecal microbiota transplantation (FMT) was conducted on C57BL/6J naïve mice for 6 weeks to receive either IH or room air (RA) fecal slurry with or without probiotics (VSL3). In addition to 16S rRNA amplicon sequencing of their GM, FMT recipients underwent arterial blood pressure (aBP) and coronary artery and aorta function testing, and their trimethylamine N-oxide (TMAO) and plasma acetate levels were determined. Finally, C57BL/6J mice were exposed to IH, IH treated with VSL3, or RA for 6 weeks, and assessed aBP and coronary artery function.

Results: GM taxonomic profiles correctly segregated IH from RA in FMT mice, and the normalizing effect of probiotics emerged. Furthermore, IH-FMT mice exhibited increased aBP and TMAO levels, and impairments in aortic and coronary artery function ($p<0.05$) that were abrogated by probiotic administration. Lastly, Treatment with VSL3 under IH conditions did not attenuate elevations in aBP or CAD.

Conclusions: Thus, GM alterations induced by chronic IH underlie, at least partially, the typical cardiovascular disturbances of sleep apnea, and can be mitigated by concurrent administration of probiotics.

Plain language summary:

Using a well-established mouse model of sleep apnea consisting of long-term intermittent hypoxia (IH), we show that the adverse cardiovascular effects of IH can be recapitulated in naïve mice receiving fecal material from IH exposed mice and that co-administration of probiotics markedly improves those cardiovascular outcomes. Thus, probiotics may serve as adjuvant treatment of sleep apnea to potentially mitigate sleep apnea-associated cardiovascular disease.

INTRODUCTION

Obstructive sleep apnea (OSA) is a chronic and extremely frequent condition that has been estimated to affect nearly a billion people around the world [1]. OSA is characterized by recurrent partial or complete upper airway obstruction during sleep, and can result in intermittent hypoxia (IH) [2]. These recurrent events over long periods of time can induce and propagate pathological processes, including endothelial dysfunction, which is a critical effector of cardiovascular disease (CVD) [3, 4]. The prevalence of OSA is as high as 40-80% in patients with CVD, including ischemic stroke and coronary artery disease (CAD) [5]. Despite these strong associations, interventional trials based on continuous airway positive pressure (CPAP) as the treatment modality have inconsistently detected the anticipated improvements in CVD, suggesting the need for adjuvant therapies aimed at the core disturbances induced by the disease [6, 7]. To address these issues, multiple studies using animal models of OSA, especially consisting of IH exposures during the sleep period, reported the emergence and propagation of endothelial dysfunction and atherosclerosis in numerous rodent vascular beds [4, 8] including the coronary circulation [9].

The gut microbiome (GM) network plays many vital roles beyond digestion, including maintenance of structural integrity of the gut barrier [10]. Perturbations in the GM community can result in changes in diversity and proportion of commensal bacteria, and are attributed to various environmental factors including diet and drugs [11]. Recent evidence suggests that GM changes are associated with multiple diseases including CVD [12] and OSA [13]. Indeed, studies involving fecal microbiota transplantation (FMT), specific GM-dependent pathways and metabolites have been shown to influence host metabolism and CVD [14]. For example, increases in GM-mediated systemic Trimethylamine N-oxide (TMAO) levels adversely impact

CVD in animal models, and human studies have further corroborated such associations in CAD and hypertension [14–16]. As a corollary, interventional studies using pre- and probiotics improved cardiovascular outcomes in patients with CVD via multiple mechanisms involving gastrointestinal mucosal barrier protection, reducing systemic inflammation and TMAO levels, and increasing levels of short chain fatty acids (SCFA) [15, 16].

Similar to CVD, GM diversity and abundance are altered in OSA patients and in animals exposed to chronic IH exposures [16–19]. Indeed, fecal matter obtained from OSA patients revealed GM changes that varied with the severity of OSA, and suggested that they may underlie some of the cardiometabolic perturbations in such patients [13, 20]. Furthermore, we and others showed that in animals exposed to chronic IH pronounced alterations in gut microbiota were detected [18, 21, 22], and persisted even after IH cessation for six weeks [18]. The characteristics of IH-induced GM alterations further suggested that the changes in GM may mediate cardiometabolic disease [16, 23–25]. However, there are no studies exploring whether IH-mediated GM alterations can directly affect vascular function in the absence of concurrent IH. Therefore, we hypothesized that FMT from mice exposed to IH to naïve mice may alter their GM and impair coronary artery and aortic vascular function. Furthermore, we postulated that treatment with probiotics would prevent, or at least mitigate vascular dysfunction in naïve mice receiving IH-FMT and in mice exposed to IH.

MATERIALS AND METHODS

All experiments were approved by the Institutional Animal Care and Use Committee (IACUC) of the University of Missouri (Protocols #9586 and #9720) and performed according to the Declarations of Helsinki conventions for the use and care of animals. Male C57BL/6J mice (8-

week-old) were purchased from The Jackson Laboratory (Bar Harbor, ME, USA). Animals were housed in a controlled environment with 12 h light–dark cycles (07.00 h–19.00 h) at constant temperature (26 ± 0.2°C) with *ad libitum* access to water and food (normal chow). At the end of the experimental period, mice were euthanized using carbon dioxide (1 min) followed by cervical dislocation.

Intermittent hypoxia exposures and probiotic treatment

The IH exposure protocol used has been described in detail previously [26]. Briefly, intermittent hypoxia (IH) mice were subjected to IH for 6 weeks while room air (RA) control mice were housed in standard housing conditions and exposed to normoxic gas (n = 10/group). IH exposures included alternating 21% F_{IO2} and 6% F_{IO2}, 20 cycles h^{-1} for 12 h day^{-1} during daylight (07:00 h – 19:00 h) using a commercially available commercial system (80 × 50 × 50 cm; Oxycycler A44XO, BioSpherix, Redfield, NY, USA). The exposures recapitulate nadir oxyhemoglobin saturations in the range of 68-75%, which are the primary correlate of moderate to severe OSA in humans [27]. The mice were in normoxic conditions (21% F_{IO2}) for the rest of the day (dark period from 19.00 h–07.00 h). Mice were treated concomitantly with the probiotic VSL3 In drinking water (4 x 10^9 colony forming units). VSL3 is a commercial probiotic containing eight bacterial strains: four strains of *Lactobacillus* (*Lactobacillus acidophilus*, *Lactobacillus plantarum*, *Lactobacillus casei*, and *Lactobacillus delbrueckii* subspecies *bulgaricus*), three strains of *Bifidobacterium* (*Bifidobacterium longum*, *Bifidobacterium breve*, *Bifidobacterium infantis*), and one strain of *Streptococcus* (*Streptococcus salivarius* subspecies *thermophilus*).

Fecal Microbiota Transplantation (FMT) in Naïve Mice

Fecal pellets from mice exposed to 6 weeks of IH or RA were collected on ice daily at noon (ZT-5) for one week then transferred to -80°C until use (n=10/group). FMT was performed by oral gavage of a fecal slurry into naïve mice three times a week at ZT-5 (male C57BL/6, 8 weeks old, Jackson Lab, n=10/group) as previously described [17, 28]. To prevent cage-related effects, recipients were randomly selected from different cages and housed with non-recipient mice and the experiments were repeated twice (n=5 in each experiment) to demonstrate reproducibility. Recipient mice were fasted for 2 hours prior to FMT, and the fecal slurry was obtained daily from fecal pellets of 5 donor mice suspended by vortexing in 1 mL PBS per 100 mg of fecal matter. Fecal mixtures were then centrifuged at 500*g* for 5 min and the supernatants were collected for FMT. Each recipient mouse received 100 µl of fecal slurry by oral gavage three times a week for 6 weeks with or without VSL3 probiotics (Alfasigma, Covington, LA) in all groups: i) RA-FMT, ii) IH-FMT, iii) RA-FMT-PRO, IV) IH-FMT-PRO. VSL3 was administered with FMT and in drinking water (4×10^9 colony forming units).

16S rRNA amplicon sequencing of gut microbiota

Fecal matter from mice corresponding to IH-FMT, RA-FMT, IH-FMT-PRO, and RA-FMT-PRO conditions were collected at ZT-5 on dry ice then processed using PowerFecal kits (Qiagen, Germany) according to the manufacturer's instructions [29]. Briefly, bacterial 16S rRNA amplicons were constructed via amplification of the V4 region of the 16S rRNA gene with universal primers (U515F/806R), flanked by Illumina standard adapter sequences [30]. The final amplicon pool was evaluated using the Advanced Analytical Fragment Analyzer automated electrophoresis system, quantified using quant-iT HS dsDNA reagent kits (Invitrogen, Carlsbad, CA, USA), and diluted according to Illumina's standard protocol for sequencing on the MiSeq instrument (Ilumina, San Diego, CA, USA) as 2×250 bp paired-end reads. Primers were

designed to match the 5' ends of the forward and reverse reads. Cutadapt (https://github.com/marcelm/cutadapt) was used to remove the the primer from the 5' end of the forward read. If found, the reverse complement of the primer to the reverse read was then removed from the forward read as were all bases downstream. Thus, a forward read could be trimmed at both ends if the insert were shorter than the amplicon length. The same approach was used on the reverse read, but with the primers in the opposite roles. Read pairs were rejected if one read or the other did not match a 5' primer, and an error-rate of 0.1 was allowed. Two passes were made over each read to ensure removal of the second primer. A minimal overlap of three bp with the 3' end of the primer sequence was required for removal. The QIIME2 DADA2 plugin (version 1.10.0) was used to denoise, de-replicate, and count ASVs (amplicon sequence variants), incorporating the following parameters: 1) forward and reverse reads were truncated to 150 bases, 2) forward and reverse reads with number of expected errors higher than 2.0 were discarded, and 3) Chimeras were detected using the "consensus" method and removed. A feature table rarefied to 44,960 features per sample was used for all 16S rRNA microbiome analyses. Taxonomies were assigned to final sequences using the Silva.v138 database, using the classify-sklearn procedure. Differential abundance testing was performed using analysis of composition of microbes (ANCOM) within QIIME2 v2021.8 and ALDEx2 within R v3.6.2 [31, 32]. An EMPress plot was generated using QIIME2 v2021.8. R v3.5.1 and Biom version 2.1.7 were used in QIIME2 [33].

Blood pressure measurements

Heart rate and arterial blood pressure (aBP) were measured using the tail-cuff method by volume pressure recording (CODA system—Kent Scientific, Torrington, CT, USA) in conscious animals between ZT-5 and 6. The tail-cuff method is reliable and comparable to telemetry measurements

using an aortic catheter [34]. Mice were placed in a cylindrical holder over a warmed blanket. After 30 min of habituation, at least 8 recordings were obtained, each separated by 5 min. The mean of the lowest five values for systolic, diastolic and mean blood pressure were retained for analyses [35].

Aortic and Coronary artery function

After euthanasia, the heart was excised, and the left anterior descending (LAD) coronary artery was micro-dissected and mounted for isometric tension recordings (Danish Myo Technology, Model 630MA, Aarhus, Denmark). In the subset of mice exposed to FMT experiments, the aorta was concurrently harvested and prepared for the myograph experiments. Data were analyzed using PowerLab software (AD Instruments). Excised vessels were normalized to a tension equivalent to that experienced by the vessels in vivo at 90mmHg pressure as previously described [36] in tissue baths of warmed (37 °C), aerated (95% O2, 5% CO2), in a physiological solution (118.99 NaCl; 4.69 KCl; 1.17 $MgSO_4$; 0.03 EDTA; 2.5 $CaCl_2$; 25 $NaHCO_3$; 1.18 KH_2PO_4; 5.5 glucose). Vessel viability was assessed by exposure to 80mM KCl. Vasoconstrictor responses were assessed to incremental concentrations of thromboxane A2 analog U46619 (10^{-9}–10^{-5} M). For relaxation studies, vessels were pre-constricted with U46619 (0.1-0.3 µM), before administration of Acetylcholine (ACh) (10^{-9}-10^{-5}M) and sodium nitroprusside (SNP) (10^{-9}-10^{-5}M) [36]. Constrictor responses are presented as a percent of the max response to 80mM KCl and the vasodilator responses are presented as a percent of maximal dilation from the pre-constricted tension.

Plasma TMAO determination

Plasma levels of TMAO (50µl) were prepared and analyzed as described previously [37] using liquid chromatography-mass spectrometric multiple reaction monitoring (LC-MS MRM) (Acquity Ultra Performance Liquid Chromatography coupled with TQ-S triple-quadrupole mass spectrometry; Waters, PA) at The University of Missouri Metabolic Core. Serum (50 ul) was mixed with 350 ul methanol and 25 ul solution of labelled internal standard (10 ug/mL) in methanol. After vortex, the samples were centrifuged at 13000 g for 5 min. The clear supernatant (~350-400 uL) was recovered and analyzed on a Water TQ MS. A series of standard solutions were prepared by diluting a master solution (5 ug/mL) with methanol containing internal standard labeled TMAO solution. The final concentrations were: 0.001, 0.005, 0.01, 0.05, 0.1, 0.5, 1.0 and 5.0 ug/mL. The concentration C13 labeled internal standard is aa ug/mL. A linear calibration curve was obtained by plotting area under curve against concentration of standard solutions. LC-MS MRM analyses were performed on a Waters Xevo TQ MS coupled to a Waters Acquity UPLC system (Waters, PA). Separations of amino acids were achieved on a Waters High Strength Silica (HSS) C18 column (2.1 x 150 mm, 1.7-µm particles) using a linear gradient of mobile phase A (A: 0.1% formic acid) and B (B: methanol). The gradient condition was: B increased from 5% to 46% over 19 min, then to 90% in 0.1 min and held at 90% for 1.9 min, returned to 5% for equilibrium in 0.1 min where it was hold for another 3.9 mins. The flow rate was 0.375 mL/min and the column temperature was 40 °C. Under the current LC conditions, the retention time of TMAO and TMAO-13C3 were found to be 0.85 min. MRM analyses were performed on the Waters Xevo TQMS in positive electrospray ionization mode for TMAO/TMAO-13C3. Two transitions, i.e., one qualitative and one quantitative transition, were monitored. The transitions were auto-optimized using Waters Masslynx Intellistart program. The two transitions for TMAO were (exact mass: 75.06) were: m/z 76.1 -> m/z 42.17 (cone voltage:

26 V, collision energy: 44 eV), m/z 76.1 -> m/z 57.40 (cone voltage: 26 V, collision energy: 16 eV). For TMAO-13C3 (exact mass: 78.08), m/z 79.1 -> m/z 41.13 (cone voltage: 24 V, collision energy: 46 eV), and m/z 79.1 -> m/z 63.09 (cone voltage: 24 V, collision energy: 14 eV) were used. MS MRM data were processed using Waters TargetLynx software. Transition m/z 76.1 -> m/z 42.17 was used as the quantitative transition for TMAO and transition m/z 79.1 -> m/z 63.09 was used for TMAO-13C3.

Plasma acetate determination

Plasma acetate levels were determined using enzyme-linked immunosorbent assay (ELISA) kit according to the manufacturer protocol (Abcam, Cambridge, UK).

Statistical analysis

Data analysis was performed using MetaboAnalyst 5.0, Past4.04, Prism 9 (GraphPad, San Diego, Ca, USA), and R version 3.6.2 statistical software. One-way and Two-way ANOVA with repeated measures and Tukey *post-hoc* test, two-way PERMANOVA, and differential abundance testing were used as appropriate. Data were tested for normality using Shapiro-Wilk test and expressed as mean ± SD. A p value < 0.05 was considered as statistically significant.

RESULTS

Changes in gut microbiome composition in naïve mice subjected to FMT from mice exposed to RA and IH and treated with VSL3

To assess the causal relationship between IH-associated changes in the fecal microbiome, FMT experiments were performed. IH was associated with changes in the microbiome similar to those seen previously, and several features of the microbiome were successfully transferred via FMT

(Fig. S1). The PCoA plots shown (Fig. 1A, 1B) reveal significant differences in fecal bacterial composition in all four groups using weighted and unweighted UniFrac distances. As in other mammalian hosts, Bacteroidetes and Firmicutes were the predominant phyla, with phylum Bacteroidetes dominated by class Bacteroidia, order Bacteroidales, and phylum Firmicutes being dominated by class Clostridia, order Clostridiales (Fig. S2). The relative abundance of bacterial taxa in IH-FMT group shows higher abundance of *Lachnospiraceae* and *Ruminococcaceae* from the phylum Firmicutes and *Prevotellaceae* and *Muribaculaceae* from the phylum Bacteroidetes, when compared to the other three groups (Fig. S3, Table S1**)**. Two separate tools, ANCOM and ALDEx2, were used in tandem to test for differences in ASV relative abundance between groups. Fig. S1 shows a cladogram of all ASVs detected among the four groups, with concentric outer circles indicating the strength of the differences detected using those methods. ASVs identified as differentially abundant between groups included two taxa present in VSL3 (Fig. 1C). Treatment with VSL3 resulted in a higher abundance of *Lactococcus* and *Bifidobacterium* species, which were noted in both RA-FMT-PRO and IH-FMT-PRO groups (Fig. 1C, Table S1) relative to IH-FMT. Thus, FMT procedures using different fecal GM as obtained from IH-exposed and RA-exposed mice altered the GM of naïve mice to recapitulate the previously documented differences in GM induced by IH [17]. Furthermore, treatment with VSL3 prevented the selective increases in bacteria abundance induced by FMT from IH mice, and increased abundance of the putatively beneficial bacteria.

VSL3 treatment normalizes elevated blood pressure in naïve mice receiving FMT from IH exposed mice

IH-FMT induced elevations of systolic (122 ± 10 mmHg), diastolic (93± 9 mmHg) and mean (102 ± 10 mmHg) blood pressure values, and such changes were abrogated by VSL3 treatment

(systolic BP: 107 ± 8 mmHg, p = 0.004; diastolic BP: 83 ± 5 mmHg, p = 0.02; mean BP: 91 ± 6 mmHg, p = 0.02, all p values *vs*. IH-FMT; Fig. 2A-2C). aBP values in RA FMT and RA-FMT-PRO experimental groups were also significantly lower when compared to IH-FMT but were similar to those obtained in IH-FMT-PRO treated animals.

VSL3 treatment mitigates coronary artery dysfunction in naïve mice induced by IH-FMT

IH-FMT enhanced maximal coronary artery contractility responses to the thromboxane A2 analog U46619 (174 ± 20%) when compared to RA-FMT (141 ± 18%, p < 0.0001), and such effects were attenuated by VSL3 treatment (IH-FMT-PRO: 157 ± 13%, p = 0.02; Fig. 3A). IH-FMT impaired coronary artery endothelium-dependent relaxation responses to ACh (65 ± 9%) when compared to RA-FMT (85 ± 7%, p < 0.0001; Fig. 3B). Concurrent administration of VSL3 prevented the relaxation impairments induced IH-FMT (IH-FMT-PRO: 79 ± 9%, p < 0.0001). Similar to the coronary arteries, IH-FMT increased maximal aortic contractility responses to phenylephrine (166 ± 22%) when compared to RA-FMT (138 ± 14%, p = 0.006; Fig. S4A), while IH-FMT-PRO treated mice showed no significant differences compared to controls (IH-FMT-PRO: 131 ± 19%, p = 0.0004). Endothelium-dependent relaxation was also impaired in the aorta of the IH-FMT group (69 ± 22%) when compared to RA-FMT mice (85 ± 4%, p = 0.003; Fig. S4B) and VSL3 concurrent treatment mitigated such impairments (IH-FMT-PRO: 82 ± 4%, p = 0.04 vs. IH-FMT). Endothelium-independent relaxation responses to the nitric oxide donor sodium nitroprusside (SNP) were similar in all groups in both aortic and coronary arteries (Fig. 3C, S4C).

VSL3 treatment reduces TMAO levels in naïve mice receiving FMT from mice exposed to IH

Plasma levels of TMAO were significantly elevated in IH-FMT mice (0.43 ± 0.06 ng/ml) when compared to RA-FMT mice (0.19 ± 0.11 ng/ml, p = 0.008; Fig. 4A). Administration of VSL3 to IH-FMT-treated mice abrogated the increase in TMAO levels (IH-FMT-PRO: 0.27 ± 0.06 ng/ml, p = 0.02). However, acetate plasma concentrations were significantly lower in IH-FMT mice (1.1 ± 0.2 μM) when compared to RA-FMT mice (3.5 ± 1.3 μM, p = 0.01, Fig. 4B), but VSL3 treatment was not associated with significant improvements in acetate concentrations in IH-FMT-PRO treated mice (1.8 ± 0.6 μM, p = 0.6).

VSL3 administration does not attenuate mean BP elevations or coronary artery dysfunction in mice exposed to IH

After 6 weeks of IH exposures and co-administration of VSL3, mean BP was significantly elevated in mice exposed to IH (111 ± 6 mmHg) when compared to RA (92 ± 4 mmHg, p < 0.001) (Fig. 5A). Treatment with VSL3 had modest non-significant reductions of mean BP (IH-PRO: 105 ± 7 mmHg vs. RA, p = 0.0009). IH exposure enhanced maximal coronary artery contractility responses to the thromboxane A2 analog U46619 (182 ± 31%) when compared to RA (133 ± 14%, p < 0.0001, Fig 5B) that were not attenuated by VSL3 treatment (161 ± 28% vs. RA, p = 0.0015). Furthermore, maximal response to endothelium-dependent relaxation by ACh was abolished in coronary arteries of IH-exposed mice (63 ± 9%) in comparison with RA (85 ± 5%, p < 0.0001; Fig. 5C) and was not rescued with VSL3 administration (68 ± 13% vs. RA, p = 0.0002). Endothelium-independent relaxation responses to the nitric oxide donor sodium nitroprusside (SNP) were similar in all groups (Fig. 5D)

DISCUSSION

The present study uncovers several novel and unprecedented findings. First, we show that changes in the composition and diversity of the GM induced by IH exposures but in the absence of actual hypoxia elicits elevations in blood pressure levels and induces impairments in coronary and aortic blood vessel functions. Furthermore, such GM changes promote increases in TMAO levels in IH-FMT mice. Secondly, VSL3 probiotic administration prevents the emergence of the vascular phenotypes induced by IH-FMT and abrogates the increases in aBP. Lastly, supplementing mice exposed to IH with VSL3 does not attenuate aBP elevations nor mitigates coronary artery dysfunction. Taken together, current findings indicate that alterations in GM diversity caused by IH can singlehandedly elicit cardiovascular perturbations, even in the absence of environmental IH, and that such cardiovascular changes can be mitigated or abrogated altogether by probiotics such as VSL3. However, IH clearly incorporates additional mechanisms that are not represented exclusively by GM alterations and likely involve autonomic dysfunction, oxidative stress, and systemic inflammation.

IH- mediated hypertension and coronary artery dysfunction

Heart disease remains the main cause of death and disability in the United States according to the 2020 Heart Disease And Stroke statistics [38]. OSA is a well-recognized risk factor for CVD, independent of other commonly associated risk factors such as sex, age, obesity and hypertension [39]. Moreover, approximately 35% of OSA patients have hypertension, while an estimated 50% of patients with hypertension suffer from concomitant OSA [40, 41].. Inevitably, untreated patients with severe OSA are 2.6 times more likely to suffer incident CAD [42]. Unfortunately, the beneficial effects of current OSA therapies such as CPAP on CVD outcomes are inconsistent and fraught with scientific controversy [6, 43]. Clinical and experimental studies denote chronic IH as the most detrimental perturbation in OSA-induced hypertension and CVD

[2, 8]. Indeed, IH can induce sympathetic activation, oxidative stress, systemic inflammation, dyslipidemia and insulin resistance, all of which can contribute to elevated blood pressure, endothelial dysfunction and atherosclerosis [3, 4, 44, 45]. Multiple studies so far have reported evidence of endothelial dysfunction in animals exposed to IH, manifesting as reduced nitric oxide bioavailability, enhanced vasoconstriction, and impaired vasodilation in multiple vascular beds, including aorta, and cerebral, femoral or carotid arteries [46–49]. Only recently, our lab has demonstrated that IH can also impair coronary artery function (left anterior descending) and reduce flow velocity reserve [9]. Thereby, there is an established link between IH mimicking OSA and CAD. However, more mechanistic studies are required to elucidate the pathways underlying the effects of IH on coronary structure and function.

IH-induced GM changes

In an effort to identify potential contributors to IH-induced vascular dysfunction, we opted to explore the GM as a causal determinant of the vascular phenotype in OSA. Indeed, it is now well established that the stability and equilibrium of the GM ecosystem are essential for maintaining health, but that perturbations leading to GM alterations can induce and propagate detrimental health consequences [11]. Recent evidence suggests that OSA is associated with GM alterations in adults and children [13, 19, 50] where most of these findings reported higher Firmicutes to Bacteroides ratio and significantly lower microbial diversity and richness. Findings in mice exposed to IH for 6 weeks revealed significant alterations in GM profiles, with increases in obligate anaerobes, such as *Prevotella*, *Lachnospiraceae* and *Desulfovibrio* [51], suggesting that fluctuations in oxygen partial pressures in the gut drive such changes. Increased presence of *Desulfovibrio* has been linked to increased mucin degradation, while *Prevotrella* is strongly linked to systemic inflammation through the generation of lipopolysaccharides (LPS) [51].

Evidence from different studies shows a controversial role played by *Lachnospiraceae*, but it is plausible that the increases in are likely a response to IH as an environmental stressor [52]. In accordance with our results, other studies using IH and hypercapnia in low-density lipoprotein receptor-deficient mice (*Ldlr*$^{-/-}$) found more than 80 microbial different features, with the largest including *Lachnospiraceae* and *Clostridiaceae* families [53]. In previous work, we showed that naïve mice kept in normoxic conditions and receiving FMT from animals exposed to IH led to GM changes that were remarkably similar to those observed in mice exposed to IH, along with corresponding increases in the abundance of the aforementioned bacteria. Our current results concur with such earlier findings, indicating that FMT from IH-exposed donors is accompanied by reproducible and consistent GM changes in the recipient mice. In mice exposed to 4 weeks of sleep fragmentation (SF), another hallmark characteristic of OSA, there were GM changes that were predominantly reflected by the growth of *Ruminococcaceae and Lachnospiraceae*, and such changes were accompanied by impaired insulin sensitivity and white adipose tissue inflammation [29]. Indeed, increased GM abundance of *Ruminococcaceae and Lachnospiraceae* is associated with atherosclerotic lesions in apolipoprotein E knockout mice (*ApoE*$^{-/-)}$ fed a western diet [54]. Although these bacteria can produce SCFAs such as butyrate [55], they also contain bile acid inducible genes that encode enzymes involved in converting host primary bile acids to secondary bile acids and act on farnesoid X receptor (FXR) and G-protein-coupled receptor (TGR5) that have been implicated in atherosclerosis [56]. *Muribaculaceae* bacterium are a dominant family in the gut and are capable of degrading complex carbohydrates [57]. Although it has been reported that the timing of fecal material collection and the cyclical effects of IH and intermittent hypercapnia (IC), another hallmark of OSA, can cause dyssynchrony of the microbiome and metabolome [58], we standardize our procedures to minimize any potential

factors that introduce variance and we found relative stability of the GM after 2-4 weeks of IH exposures in our previous work. The relative changes in GM are modest from week to week if the IH exposure continues and even after 6 weeks of IH cessation we noted an incomplete recover of the GM [18]. The overall net effect of such GM changes on the intestinal permeability of IH-FMT recipients was not examined, but clearly warrants future studies, since the overall metabolomic composition of the GM may facilitate the translocation of CAD-inducing metabolites in IH-exposed and IH-FMT mice.

IH-induced GM changes and cardiovascular disturbances

Recent evidence suggests an obligatory role of microbiota in BP homeostasis. Indeed, the absence of microbiota in germ-free rats resulted with relative hypotension accompanied by marked reduction is vascular reactivity, and both were restored by the introduction of microbiota to germ-free rats [59]. The evidence linking an association between GM alterations and hypertension is much more robust in both human and animal studies [16]. Apparent differences are consistently detected between the GM of normotensive and hypertensive mice and patients [60]. Collectively, there is less microbial richness and diversity, lower abundance of SCFA-producing bacteria , all of which play a role in inducing hypertension [61]. Indeed, SCFA (e.g., acetate, butyrate) are essential for maintaining gut barrier integrity, decreasing gut wall inflammation, and most importantly, reducing aBP. Previous studies using FMT from hypertensive mice and humans to normotensive mice resulted in increased aBP levels [60]. A recent review summarized the major mechanisms underlying GM induced-cardiovascular complication of OSA being decreased abundance of SCFAs, mucin-degradation and increased inflammation [62]. In animals, following FMT from rats exposed to a procedure aimed a reproducing OSA (repetitive tracheal balloon inflations during sleep) coupled with a high fat

diet (HFD), recipient rats fed normal chow developed hypertension along with detectable changes in the GM diversity and abundance of SCFA-producing bacteria [63]. In the present study, we show that FMT from animals exposed to IH elicited elevations in systolic, diastolic, and mean arterial aBP. Furthermore, acetate levels were reduced in IH-FMT mice, which may account for the GM-induced elevations in aBP, since chronic acetate infusion in the cecum of rats exposed to a model of OSA for 2 weeks prevented the emergence of inflammation and hypertension, implicating acetate as a key player in OSA-induced hypertension [63].

Most CVD risk factors, including OSA, can induce GM alterations. The associated intestinal inflammation and intestinal barrier damage can facilitate the translocation of microbial structural components and metabolites, including TMAO, to promote the development of CVD [14]. TMAO is a product of gut microbial metabolism of TMA-containing nutrient precursors (i.e., choline) using TMA-lyases. Following transport to the liver via the portal vein, TMA is metabolized by flavin monooxygenases into TMAO [64]. Senthong *et al*. found that elevated TMAO levels were an independent predictor of diffuse CAD atherosclerotic lesions, even after adjustment for traditional risk factors [65]. Initial functional studies in mice consistently show that GM-derived TMAO increases atherosclerosis susceptibility [14]. Indeed, dietary supplementation of choline in $ApoE^{-/-}$ mice enhanced atherosclerotic lesion formation [64]. However, not all TMAO precursor feeding studies have shown similar results, suggesting that differences in host microbial composition have a substantial influence the phenotype observed [66]. Furthermore, a recent study showed that IH and IC can modulate atherosclerosis progression differently in distinct vascular beds (aorta, pulmonary artery) in $ApoE^{-/-}$ mice where IH promotes an atherosclerotic luminal gut environment [67]. Thus, it is critical to take in consideration that various models of OSA may induce changes in gut metabolome and

microbiome that can interact differently with distinct vascular beds. A study conducted by the same group showed that treatment with 3,3-dimethyl-1-butanol (DMB), an inhibitor microbial TMA lyase, reduces the size of atherosclerotic lesions enhanced in pulmonary arteries of mice exposed to IH and IC [68]. In our study, naïve mice receiving FMT from IH-exposed mice developed aortic and coronary artery endothelium-dependent relaxation impairments and enhanced vasoconstrictive responses, in addition to elevated TMAO plasma levels, thereby confirming the detrimental role of IH-induced GM alterations on endothelial function in the absence of IH. Furthermore, the elevated levels of TMAO despite normal chow diet suggests increased abundance of TMA-producing bacteria. Other modulators of atherosclerosis impacted by GM alterations are bile acids [69]. Several bile acids have proinflammatory and proatherogenic activities such as deoxycholic acid (DCA) and tauro-β-muricholic acid (TβMCA) and have been shown to increase in animal models of OSA [58, 67]. However, whether endothelial dysfunction in IH-FMT mice resulted from elevated TMAO levels, aBP elevation, or a combination thereof remains to be explored and the role of bile acids should be explored.

Probiotics effects on GM-mediated cardiovascular disturbances

Probiotics refer to species of live bacteria that confer beneficial health effects on the host when ingested in adequate amounts can exert a wide range of beneficial effects, such as inhibiting colonization by pathogenic bacteria and reinforcing the mucosal barrier [70]. The relatively insufficient effectiveness of pharmaceutical interventions for the management of atherosclerosis and CVD, combined with the recent advances in understanding and recognizing GM - host interactions have generated substantial interest in probiotics as a potential add-ons therapy for CVD [71]. Supplementation with probiotics significantly improved markers of CAD, including nitric oxide, inflammation and oxidative stress [72]. One study reported that supplementation

with *Lactobacillus plantarum* 299v ameliorated vascular endothelial dysfunction and inflammation in men with CAD [73]. In animals, probiotic supplementation with VSL3 or *Lactobacillus plantarum* ZDY04 reduced high HFD-induced lesion development in ApoE$^{-/-}$ mice along with reduced vascular inflammation, adhesion molecules, plasma TMAO, and TMAO-induced atherosclerosis [74],[75]. VSL3 supplementation attenuated oxidative stress-mediated endothelial dysfunction in rat mesenteric arteries following bile duct ligation [76]. These data suggest that probiotics, such as VSL3, have the potential to ameliorate vascular dysfunction in atherosclerotic disease. In OSA rats fed HFD, administration of SCFA replenishing probiotic *C. butyricum* and the prebiotic Hylon VII increased the relative abundance of SCFA-producing bacteria and reduced elevated BP [63]. Another study in OSA rats fed HFD treated with *Lactobacillus rhamnosus* probiotic showed that TMAO levels, inflammatory cytokines, and hypertension severity were all reduced [77]. Lastly, mice exposed to IH and fed HFD with high fructose diet for 12 weeks had significant cardiac morphological changes, cardiac dysfunction, cardiac collagen accumulation and increased cardiac inflammation and oxidative stress that were all prevented by administration of *Lactobacillus rhamnosus GG* [78]. In our study, VSL3 supplementation prevented the elevations in aBP and TMAO levels and attenuated aortic and coronary artery endothelial dysfunction in naïve mice receiving FMT from IH-exposed animals. Thus, targeted probiotic supplementation exerts protective effects against GM alteration-induced CAD in the context of IH mimicking OSA. However, despite treating mice exposed to IH with VSL3, only modest decreases in aBP were noticed with no improvements in coronary artery function. Despite the positive results in our FMT experiments and previous pre- and probiotic treatments in other murine models of OSA, it is predictable that VSL3 treatment was insufficient to protect against the plethora of adverse pathological stimuli induced by chronic IH including

excessive sympathetic innervation, oxidative stress, inflammation, and metabolic dysregulation [4, 79].

Our study has several limitations; firstly, only young lean C57Bl/6 mice were studied, and the effect of age, sex and obesity were not evaluated despite having great clinical relevancy. Secondly, recent evidence points to potential role of upper and lower respiratory microbiota modulation in OSA and its correlation with multiple pathologies. This study lacks the characterization of this microbiota which may have potentially influenced the outcomes [80–82]. Thirdly, the study lacks comprehensive metabolomic assessments that may reveal microbial metabolic pathways and identifying specific metabolites involved in IH-induced CAD. However, the study of the microbiome in the context of OSA is still in the early stages and our study contributes to the field of OSA and CVD.

In conclusion, FMT from mice exposed to IH simulating OSA into naïve mice recapitulates IH systemic aBP elevations and vascular perturbations in naïve recipient mice in the absence of IH exposures. Thus, a causal link emerges between IH-induced GM alterations and vascular dysfunction affecting both aortic and coronary arteries. Furthermore, probiotic administration prevents the detrimental cardiovascular phenotype in IH FMT recipient mice despite the modest attenuation observed in IH-exposed mice. The data indicates an integral role of GM as a one modulator, but not the only modulator of OSA-induced CAD and suggests probiotics as a form of targeted adjuvant therapy in patients with OSA.

Acknowledgments

This work was supported by the use of facilities and resources at the Harry S Truman Memorial Veteran’s Hospital in Columbia, MO. We would like to thank Dr. Zhanghong Qiao (Child

Health, University of Missouri) for his assistance in the FMT studies, and Drs. Luis Martinez-Lemus (Medical Physiology and Pharmacology) and Jaume Padilla (Nutrition and Exercise Physiology, University of Missouri) for allowing us the use of the aBP measuring system.

Authors' contributions

M. Badran, A. Khalyfa, S. Bender and A. Ericsson performed experiments. M. Badran and A. Ericsson analyzed data. M. Badran wrote the paper. D. Gozal provided the conceptual framework and continuous guidance for the project, and critically reviewed and revised the manuscript. All authors reviewed and approved the contents of the manuscript.

Funding and support

This study was supported in part by NIH grants HL130984, HL140548, and G061824 and by a Tier 2 Grant from the University of Missouri.

Data and materials availability

Custom script used to analyze 16S rRNA amplicon sequencing data are available at [https://github.com/ericsson-lab/IH_RA_FMT]. All sequencing data have been uploaded to the NCBI Sequence Read Archive (SRA), and a SRA BioProject accession number is pending

References

1. Benjafield A V., Ayas NT, Eastwood PR, Heinzer R, Ip MSM, Morrell MJ, Nunez CM,

Patel SR, Penzel T, Pépin JLD, Peppard PE, Sinha S, Tufik S, Valentine K, Malhotra A, M, et al. Estimation of the global prevalence and burden of obstructive sleep apnoea: a literature-based analysis. Lancet. Respir. Med. 2019; 7: 687–698 Available from: https://pubmed.ncbi.nlm.nih.gov/31300334/.

2. Badran M, Yassin BA, Fox N, Laher I, Ayas N. Epidemiology of Sleep Disturbances and Cardiovascular Consequences. Can. J. Cardiol. 2015; 7: p. 873–879 Available from: https://pubmed.ncbi.nlm.nih.gov/26037823/.

3. Badran M, Ayas N, Laher I. Cardiovascular complications of sleep apnea: Role of oxidative stress. Oxid. Med. Cell. Longev. 2014; 2: 985285 Available from: https://pubmed.ncbi.nlm.nih.gov/24734153/.

4. Badran M, Ayas N, Laher I. Insights into obstructive sleep apnea research. Sleep Med. 2014; 5: p. 485–495 Available from: https://pubmed.ncbi.nlm.nih.gov/24824769/.

5. Javaheri S, Barbe F, Campos-Rodriguez F, Dempsey JA, Khayat R, Javaheri S, Malhotra A, Martinez-Garcia MA, Mehra R, Pack AI, Polotsky VY, Redline S, Somers VK. Sleep Apnea: Types, Mechanisms, and Clinical Cardiovascular Consequences J. Am. Coll. Cardiol. p. 841–858Available from: https://pubmed.ncbi.nlm.nih.gov/28209226/.

6. Sánchez-de-la-Torre M, Sánchez-de-la-Torre A, Bertran S, Abad J, Duran-Cantolla J, Cabriada V, Mediano O, Masdeu MJ, Alonso ML, Masa JF, Barceló A, de la Peña M, Mayos M, Coloma R, Montserrat JM, Chiner E, Perelló S, Rubinós G, Mínguez O, Pascual L, Cortijo A, Martínez D, Aldomà A, Dalmases M, McEvoy RD, Barbé F, Abad L, Muñoz A, Zamora E, Vicente I, et al. Effect of obstructive sleep apnoea and its treatment with continuous positive airway pressure on the prevalence of cardiovascular

events in patients with acute coronary syndrome (ISAACC study): a randomised controlled trial. *Lancet Respir. Med.* [Internet] Lancet Publishing Group; 2020 [cited 2020 Sep 25]; 8: 359–367Available from: https://pubmed.ncbi.nlm.nih.gov/31839558/.

7. Labarca G, Dreyse J, Drake L, Jorquera J, Barbe F. Efficacy of continuous positive airway pressure (CPAP) in the prevention of cardiovascular events in patients with obstructive sleep apnea: Systematic review and meta-analysis [Internet]. Sleep Med. Rev. Sleep Med Rev; 2020 [cited 2021 Sep 20]. p. 101312Available from: https://pubmed.ncbi.nlm.nih.gov/32248026/.

8. Harki O, Boete Q, Pépin J-L, Arnaud C, Belaidi E, Faury G, Khouri C, Briançon-Marjollet A. Intermittent hypoxia-related alterations in vascular structure and function: a systematic review and meta-analysis of rodent data. *Eur. Respir. J.* [Internet] European Respiratory Society; 2021 [cited 2021 Sep 17]; : 2100866Available from: https://erj.ersjournals.com/content/early/2021/07/29/13993003.00866-2021.

9. Badran M, Bender SB, Khalyfa A, Padilla J, Martinez-Lemus LA, Gozal D. Temporal Changes in Coronary Artery Function and Flow Velocity Reserve in Mice Exposed to Chronic Intermittent Hypoxia. *Sleep* [Internet] Sleep; 2022 [cited 2022 Jul 11]; Available from: https://pubmed.ncbi.nlm.nih.gov/35661901/.

10. Jandhyala SM, Talukdar R, Subramanyam C, Vuyyuru H, Sasikala M, Reddy DN. Role of the normal gut microbiota. *World J. Gastroenterol.* [Internet] Baishideng Publishing Group Inc; 2015 [cited 2021 Aug 4]; 21: 8836–8847Available from: /pmc/articles/PMC4528021/.

11. Shreiner AB, Kao JY, Young VB. The gut microbiome in health and in disease [Internet].

Curr. Opin. Gastroenterol. NIH Public Access; 2015 [cited 2021 Sep 15]. p. 69–75Available from: /pmc/articles/PMC4290017/.

12. Brown JM, Hazen SL. The gut microbial endocrine organ: Bacterially derived signals driving cardiometabolic diseases. *Annu. Rev. Med.* [Internet] Annu Rev Med; 2015 [cited 2021 Sep 1]; 66: 343–359Available from: https://pubmed.ncbi.nlm.nih.gov/25587655/.

13. Ko CY, Liu QQ, Su HZ, Zhang HP, Fan JM, Yang JH, Hu AK, Liu YQ, Chou D, Zeng YM. Gut microbiota in obstructive sleep apnea–hypopnea syndrome: Disease-related dysbiosis and metabolic comorbidities. *Clin. Sci.* [Internet] Portland Press Ltd; 2019 [cited 2020 May 12]; 133: 905–917Available from: http://www.ncbi.nlm.nih.gov/pubmed/30957778.

14. Witkowski M, Weeks TL, Hazen SL. Gut Microbiota and Cardiovascular Disease [Internet]. Circ. Res. Lippincott Williams & Wilkins Hagerstown, MD; 2020 [cited 2021 Sep 16]. p. 553–570Available from: https://www.ahajournals.org/doi/abs/10.1161/CIRCRESAHA.120.316242.

15. Badran M, Mashaqi S, Gozal D. herapeutic interventions targeting human microbiome as a novel therapy for obstructive sleep apnea – A literature review. *Expert Opin. Ther. Targets* 2020; .

16. Mashaqi S, Gozal D. Obstructive sleep apnea and systemic hypertension: Gut dysbiosis as the mediator? J. Clin. Sleep Med. American Academy of Sleep Medicine; 2019. p. 1517–1527.

17. Badran M, Khalyfa A, Ericsson A, Gozal D. Fecal microbiota transplantation from mice exposed to chronic intermittent hypoxia elicits sleep disturbances in naïve mice [Internet].

Exp. Neurol. Academic Press Inc.; 2020 [cited 2020 Oct 7].Available from: https://pubmed.ncbi.nlm.nih.gov/32835671/.

18. Moreno-Indias I, Torres M, Sanchez-Alcoholado L, Cardona F, Almendros I, Gozal D, Montserrat JM, Queipo-Ortuño MI, Farré R. Normoxic recovery mimicking treatment of sleep apnea does not reverse intermittent hypoxia-induced bacterial dysbiosis and low-grade endotoxemia in mice. *Sleep* Oxford University Press (OUP); 2016; 39: 1891–1897.

19. Kheirandish-Gozal L, Peris E, Wang Y, Kakazu MT, Khalyfa A, Carreras A, Goza D. Lipopolysaccharide-Binding protein plasma levels in children: Effects of obstructive sleep apnea and obesity. *J. Clin. Endocrinol. Metab.* [Internet] 2014 [cited 2020 May 13]; 99: 656–663Available from: http://www.ncbi.nlm.nih.gov/pubmed/24276451.

20. Ko CY, Fan JM, Hu AK, Su HZ, Yang JH, Huang LM, Yan FR, Zhang HP, Zeng YM. Disruption of sleep architecture in Prevotella enterotype of patients with obstructive sleep apnea-hypopnea syndrome. *Brain Behav.* John Wiley and Sons Ltd; 2019; 9.

21. Tripathi A, Xu ZZ, Xue J, Poulsen O, Gonzalez A, Humphrey G, Meehan MJ, Melnik A V., Ackermann G, Zhou D, Malhotra A, Haddad GG, Dorrestein PC, Knight R. Intermittent Hypoxia and Hypercapnia Reproducibly Change the Gut Microbiome and Metabolome across Rodent Model Systems. *mSystems* American Society for Microbiology; 2019; 4.

22. Lucking EF, O'Connor KM, Strain CR, Fouhy F, Bastiaanssen TFS, Burns DP, Golubeva A V., Stanton C, Clarke G, Cryan JF, O'Halloran KD. Chronic intermittent hypoxia disrupts cardiorespiratory homeostasis and gut microbiota composition in adult male guinea-pigs. *EBioMedicine* Elsevier B.V.; 2018; 38: 191–205.

23. Farré N, Farré R, Gozal D. Sleep Apnea Morbidity: A Consequence of Microbial-Immune Cross-Talk? *Chest* Elsevier Inc; 2018; 154: 754–759.

24. Hu C, Wang P, Yang Y, Li J, Jiao X, Yu H, Wei Y, Li J, Qin Y. Chronic Intermittent Hypoxia Participates in the Pathogenesis of Atherosclerosis and Perturbs the Formation of Intestinal Microbiota. *Front. Cell. Infect. Microbiol.* Frontiers; 2021; 11: 392.

25. Zhou D, Xue J, Miyamoto Y, Poulsen O, Eckmann L, Haddad GG. Microbiota Modulates Cardiac Transcriptional Responses to Intermittent Hypoxia and Hypercapnia. *Front. Physiol.* Frontiers; 2021; 12: 864.

26. Carreras A, Kayali F, Zhang J, Hirotsu C, Wang Y, Gozal D. Metabolic effects of intermittent hypoxia in mice: Steady versus high-frequency applied hypoxia daily during the rest period. *Am. J. Physiol. - Regul. Integr. Comp. Physiol.* [Internet] Am J Physiol Regul Integr Comp Physiol; 2012 [cited 2021 Sep 17]; 303Available from: https://pubmed.ncbi.nlm.nih.gov/22895743/.

27. Farré R, Montserrat JM, Gozal D, Almendros I, Navajas D. Intermittent hypoxia severity in animal models of sleep apnea. *Front. Physiol.* [Internet] Frontiers Media S.A.; 2018 [cited 2020 May 15]; 9Available from: https://pubmed.ncbi.nlm.nih.gov/30459638/.

28. Khalyfa A, Ericsson A, Qiao Z, Almendros I, Farré R, Gozal D. Circulating exosomes and gut microbiome induced insulin resistance in mice exposed to intermittent hypoxia: Effects of physical activity. *EBioMedicine* [Internet] EBioMedicine; 2021 [cited 2021 Sep 20]; 64Available from: https://pubmed.ncbi.nlm.nih.gov/33485839/.

29. Poroyko VA, Carreras A, Khalyfa A, Khalyfa AA, Leone V, Peris E, Almendros I, Gileles-Hillel A, Qiao Z, Hubert N, Farré R, Chang EB, Gozal D. Chronic Sleep

Disruption Alters Gut Microbiota, Induces Systemic and Adipose Tissue Inflammation and Insulin Resistance in Mice. *Sci. Rep.* Nature Publishing Group; 2016; 6: 1–11.

30. Caporaso JG, Lauber CL, Walters WA, Berg-Lyons D, Lozupone CA, Turnbaugh PJ, Fierer N, Knight R. Global patterns of 16S rRNA diversity at a depth of millions of sequences per sample. *Proc. Natl. Acad. Sci. U. S. A.* National Academy of Sciences; 2011; 108: 4516–4522.

31. Fernandes AD, Reid JNS, Macklaim JM, McMurrough TA, Edgell DR, Gloor GB. Unifying the analysis of high-throughput sequencing datasets: Characterizing RNA-seq, 16S rRNA gene sequencing and selective growth experiments by compositional data analysis. *Microbiome* [Internet] BioMed Central; 2014 [cited 2021 Dec 23]; 2: 15Available from: /pmc/articles/PMC4030730/.

32. Mandal S, Van Treuren W, White RA, Eggesbø M, Knight R, Peddada SD. Analysis of composition of microbiomes: a novel method for studying microbial composition. *Microb. Ecol. Heal. Dis.* [Internet] Microb Ecol Health Dis; 2015 [cited 2021 Dec 23]; 26: 3402Available from: https://pubmed.ncbi.nlm.nih.gov/26028277/.

33. Cantrell K, Fedarko MW, Rahman G, McDonald D, Yang Y, Zaw T, Gonzalez A, Janssen S, Estaki M, Haiminen N, Beck KL, Zhu Q, Sayyari E, Morton JT, Armstrong G, Tripathi A, Gauglitz JM, Marotz C, Matteson NL, Martino C, Sanders JG, Carrieri AP, Song SJ, Swafford AD, Dorrestein PC, Andersen KG, Parida L, Kim H-C, Vázquez-Baeza Y, Knight R. EMPress Enables Tree-Guided, Interactive, and Exploratory Analyses of Multi-omic Data Sets. *mSystems* [Internet] American Society for Microbiology (ASM); 2021 [cited 2021 Dec 23]; 6: e01216-20Available from: /pmc/articles/PMC8546999/.

34. Feng M, Whitesall S, Zhang Y, Beibel M, D'Alecy L, DiPetrillo K. Validation of volume-pressure recording tail-cuff blood pressure measurements. *Am. J. Hypertens.* [Internet] Am J Hypertens; 2008 [cited 2020 Sep 25]; 21: 1288–1291Available from: https://pubmed.ncbi.nlm.nih.gov/18846043/.

35. Elliot-Portal E, Laouafa S, Arias-Reyes C, Janes TA, Joseph V, Soliz J. Brain-derived erythropoietin protects from intermittent hypoxia-induced cardiorespiratory dysfunction and oxidative stress in mice. *Sleep* [Internet] Oxford University Press; 2018 [cited 2020 Sep 25]; 41Available from: https://pubmed.ncbi.nlm.nih.gov/29697839/.

36. Mueller KB, Bender SB, Hong K, Yang Y, Aronovitz M, Jaisser F, Hill MA, Jaffe IZ. Endothelial mineralocorticoid receptors differentially contribute to coronary and mesenteric vascular function without modulating blood pressure. *Hypertension* [Internet] Lippincott Williams and Wilkins; 2015 [cited 2020 Sep 25]; 66: 988–997Available from: https://pubmed.ncbi.nlm.nih.gov/26351033/.

37. Ufnal M, Jazwiec R, Dadlez M, Drapala A, Sikora M, Skrzypecki J. Trimethylamine-N-Oxide: A Carnitine-Derived Metabolite That Prolongs the Hypertensive Effect of Angiotensin II in Rats. *Can. J. Cardiol.* [Internet] Can J Cardiol; 2014 [cited 2021 Sep 22]; 30: 1700–1705Available from: https://pubmed.ncbi.nlm.nih.gov/25475471/.

38. Virani SS, Alonso A, Benjamin EJ, Bittencourt MS, Callaway CW, Carson AP, Chamberlain AM, Chang AR, Cheng S, Delling FN, Djousse L, Elkind MSV, Ferguson JF, Fornage M, Khan SS, Kissela BM, Knutson KL, Kwan TW, Lackland DT, Lewis TT, Lichtman JH, Longenecker CT, Loop MS, Lutsey PL, Martin SS, Matsushita K, Moran AE, Mussolino ME, Perak AM, Rosamond WD, et al. Heart disease and stroke statistics—

2020 update: A report from the American Heart Association [Internet]. Circulation Lippincott Williams and Wilkins; 2020 [cited 2020 Sep 25]. p. E139–E596Available from: https://pubmed.ncbi.nlm.nih.gov/31992061/.

39. Dorasamy P. Obstructive sleep apnea and cardiovascular risk [Internet]. Ther. Clin. Risk Manag. Dove Press; 2007Available from: /pmc/articles/PMC2387304/.

40. Silverberg DS, Oksenberg A, Laina A. Sleep-related breathing disorders as a major cause of essential hypertension: Fact or fiction? [Internet]. Curr. Opin. Nephrol. Hypertens. Curr Opin Nephrol Hypertens; 1998 [cited 2021 Sep 15]. p. 353–357Available from: https://pubmed.ncbi.nlm.nih.gov/9690031/.

41. Pedrosa RP, Drager LF, Gonzaga CC, Sousa MG, De Paula LKG, Amaro ACS, Amodeo C, Bortolotto LA, Krieger EM, Bradley TD, Lorenzi-Filho G. Obstructive sleep apnea: The most common secondary cause of hypertension associated with resistant hypertension. *Hypertension* [Internet] Hypertension; 2011 [cited 2021 Sep 15]; 58: 811–817Available from: https://pubmed.ncbi.nlm.nih.gov/21968750/.

42. Hla KM, Young T, Hagen EW, Stein JH, Finn LA, Nieto FJ, Peppard PE. Coronary heart disease incidence in sleep disordered breathing: The Wisconsin Sleep Cohort Study. *Sleep* [Internet] Sleep; 2015 [cited 2021 Sep 10]; 38: 677–684Available from: https://pubmed.ncbi.nlm.nih.gov/25515104/.

43. McEvoy RD, Antic NA, Heeley E, Luo Y, Ou Q, Zhang X, Mediano O, Chen R, Drager LF, Liu Z, Chen G, Du B, McArdle N, Mukherjee S, Tripathi M, Billot L, Li Q, Lorenzi-Filho G, Barbe F, Redline S, Wang J, Arima H, Neal B, White DP, Grunstein RR, Zhong N, Anderson CS. CPAP for Prevention of Cardiovascular Events in Obstructive Sleep

Apnea. *N. Engl. J. Med.* [Internet] Massachussetts Medical Society; 2016 [cited 2020 Sep 25]; 375: 919–931Available from: https://pubmed.ncbi.nlm.nih.gov/27571048/.

44. Castro-Grattoni AL, Alvarez-Buvé R, Torres M, Farré R, Montserrat JM, Dalmases M, Almendros I, Barbé F, Sánchez-De-La-Torre M. Intermittent Hypoxia-Induced Cardiovascular Remodeling Is Reversed by Normoxia in a Mouse Model of Sleep Apnea. *Chest* [Internet] Elsevier B.V.; 2016 [cited 2020 Sep 25]; 149: 1400–1408Available from: https://pubmed.ncbi.nlm.nih.gov/26836908/.

45. Trzepizur W, Cortese R, Gozal D. Murine models of sleep apnea: functional implications of altered macrophage polarity and epigenetic modifications in adipose and vascular tissues [Internet]. Metabolism. W.B. Saunders; 2018 [cited 2020 Sep 29]. p. 44–55Available from: https://pubmed.ncbi.nlm.nih.gov/29154950/.

46. Durgan DJ, Crossland RF, Lloyd EE, Phillips SC, Bryan RM. Increased cerebrovascular sensitivity to endothelin-1 in a rat model of obstructive sleep apnea: A role for endothelin receptor B. *J. Perinatol.* [Internet] J Cereb Blood Flow Metab; 2015 [cited 2021 Sep 18]; 35: 402–411Available from: https://pubmed.ncbi.nlm.nih.gov/25425077/.

47. Krause BJ, Casanello P, Dias AC, Arias P, Velarde V, Arenas GA, Preite MD, Iturriaga R. Chronic intermittent hypoxia-induced vascular dysfunction in rats is reverted by N-acetylcysteine supplementation and arginase inhibition. *Front. Physiol.* [Internet] Front Physiol; 2018 [cited 2021 Sep 18]; 9Available from: https://pubmed.ncbi.nlm.nih.gov/30087615/.

48. Campen MJ, Shimoda LA, O'Donnell CP. Acute and chronic cardiovascular effects of intermittent hypoxia in C57BL/6J mice. *J. Appl. Physiol.* [Internet] J Appl Physiol (1985);

2005 [cited 2021 Sep 18]; 99: 2028–2035Available from: https://pubmed.ncbi.nlm.nih.gov/16002771/.

49. Yang Q, Liang Q, Balakrishnan B, Belobrajdic DP, Feng QJ, Zhang W. Role of dietary nutrients in the modulation of gut microbiota: A narrative review. Nutrients MDPI AG; 2020.

50. Valentini F, Evangelisti M, Arpinelli M, Di Nardo G, Borro M, Simmaco M, Villa MP. Gut microbiota composition in children with obstructive sleep apnoea syndrome: a pilot study. *Sleep Med.* [Internet] Sleep Med; 2020 [cited 2022 Jul 11]; 76: 140–147Available from: https://pubmed.ncbi.nlm.nih.gov/33181474/.

51. Moreno-Indias I, Torres M, Montserrat JM, Sanchez-Alcoholado L, Cardona F, Tinahones FJ, Gozal D, Poroyko VA, Navajas D, Queipo-Ortuño MI, Farré R. Intermittent hypoxia alters gut microbiota diversity in a mouse model of sleep apnoea. *Eur. Respir. J.* [Internet] European Respiratory Society; 2015 [cited 2020 May 12]; 45: 1055–1065Available from: http://www.ncbi.nlm.nih.gov/pubmed/25537565.

52. Vacca M, Celano G, Calabrese FM, Portincasa P, Gobbetti M, De Angelis M. The controversial role of human gut lachnospiraceae [Internet]. Microorganisms Multidisciplinary Digital Publishing Institute (MDPI); 2020 [cited 2021 Sep 14].Available from: /pmc/articles/PMC7232163/.

53. Tripathi A, Melnik A V., Xue J, Poulsen O, Meehan MJ, Humphrey G, Jiang L, Ackermann G, McDonald D, Zhou D, Knight R, Dorrestein PC, Haddad GG. Intermittent Hypoxia and Hypercapnia, a Hallmark of Obstructive Sleep Apnea, Alters the Gut Microbiome and Metabolome. *mSystems* American Society for Microbiology; 2018; 3.

54. Liu B, Zhang Y, Wang R, An Y, Gao W, Bai L, Li Y, Zhao S, Fan J, Liu E. Western diet feeding influences gut microbiota profiles in apoE knockout mice. *Lipids Health Dis.* [Internet] Lipids Health Dis; 2018 [cited 2021 Sep 14]; 17Available from: https://pubmed.ncbi.nlm.nih.gov/30021609/.

55. Ohira H, Tsutsui W, Fujioka Y. Are Short Chain Fatty Acids in Gut Microbiota Defensive Players for Inflammation and Atherosclerosis? *J. Atheroscler. Thromb.* [Internet] J Atheroscler Thromb; 2017 [cited 2022 Jul 12]; 24: 660–672Available from: https://pubmed.ncbi.nlm.nih.gov/28552897/.

56. Miyazaki-Anzai S, Masuda M, Kohno S, Levi M, Shiozaki Y, Keenan AL, Miyazaki M. Simultaneous inhibition of FXR and TGR5 exacerbates atherosclerotic formation. *J. Lipid Res.* [Internet] J Lipid Res; 2018 [cited 2022 Jul 12]; 59: 1709–1713Available from: https://pubmed.ncbi.nlm.nih.gov/29976576/.

57. Seedorf H, Griffin NW, Ridaura VK, Reyes A, Cheng J, Rey FE, Smith MI, Simon GM, Scheffrahn RH, Woebken D, Spormann AM, Van Treuren W, Ursell LK, Pirrung M, Robbins-Pianka A, Cantarel BL, Lombard V, Henrissat B, Knight R, Gordon JI. Bacteria from diverse habitats colonize and compete in the mouse gut. *Cell* [Internet] Cell; 2014 [cited 2022 Jul 12]; 159: 253–266Available from: https://pubmed.ncbi.nlm.nih.gov/25284151/.

58. Allaband C, Lingaraju A, Martino C, Russell B, Tripathi A, Poulsen O, Dantas Machado AC, Zhou D, Xue J, Elijah E, Malhotra A, Dorrestein PC, Knight R, Haddad GG, Zarrinpar A. Intermittent Hypoxia and Hypercapnia Alter Diurnal Rhythms of Luminal Gut Microbiome and Metabolome. *mSystems* [Internet] mSystems; 2021 [cited 2022 Jul

12]; 6Available from: https://pubmed.ncbi.nlm.nih.gov/34184915/.

59. Joe B, McCarthy CG, Edwards JM, Cheng X, Chakraborty S, Yang T, Golonka RM, Mell B, Yeo JY, Bearss NR, Furtado J, Saha P, Yeoh BS, Vijay-Kumar M, Wenceslau CF. Microbiota Introduced to Germ-Free Rats Restores Vascular Contractility and Blood Pressure. *Hypertens. (Dallas, Tex. 1979)* [Internet] Hypertension; 2020 [cited 2022 Jul 12]; 76: 1847–1855Available from: https://pubmed.ncbi.nlm.nih.gov/33070663/.

60. Adnan S, Nelson JW, Ajami NJ, Venna VR, Petrosino JF, Bryan RM, Durgan DJ. Alterations in the gut microbiota can elicit hypertension in rats. *Physiol. Genomics* [Internet] Physiol Genomics; 2017 [cited 2020 Jul 21]; 49: 96–104Available from: https://pubmed.ncbi.nlm.nih.gov/28011881/.

61. Li J, Zhao F, Wang Y, Chen J, Tao J, Tian G, Wu S, Liu W, Cui Q, Geng B, Zhang W, Weldon R, Auguste K, Yang L, Liu X, Chen L, Yang X, Zhu B, Cai J. Gut microbiota dysbiosis contributes to the development of hypertension. *Microbiome* [Internet] BioMed Central Ltd.; 2017 [cited 2020 Jul 21]; 5Available from: https://pubmed.ncbi.nlm.nih.gov/28143587/.

62. Zhang X, Wang S, Xu H, Yi H, Guan J, Yin S. Metabolomics and microbiome profiling as biomarkers in obstructive sleep apnoea: a comprehensive review. *Eur. Respir. Rev.* [Internet] Eur Respir Rev; 2021 [cited 2022 Jul 12]; 30Available from: https://pubmed.ncbi.nlm.nih.gov/33980666/.

63. Ganesh BP, Nelson JW, Eskew JR, Ganesan A, Ajami NJ, Petrosino JF, Bryan RM, Durgan DJ. Prebiotics, probiotics, and acetate supplementation prevent hypertension in a model of obstructive sleep apnea. *Hypertension* [Internet] Lippincott Williams and

Wilkins; 2018 [cited 2020 Jul 21]; 72: 1141–1150Available from: https://pubmed.ncbi.nlm.nih.gov/30354816/.

64. Wang Z, Klipfell E, Bennett BJ, Koeth R, Levison BS, Dugar B, Feldstein AE, Britt EB, Fu X, Chung YM, Wu Y, Schauer P, Smith JD, Allayee H, Tang WHW, Didonato JA, Lusis AJ, Hazen SL. Gut flora metabolism of phosphatidylcholine promotes cardiovascular disease. *Nature* [Internet] Nature Publishing Group; 2011 [cited 2021 Sep 16]; 472: 57–65Available from: https://www.nature.com/articles/nature09922.

65. Senthong V, Li XS, Hudec T, Couglin J, Wu Y, Levison B, Wang Z, Hazen SL, Wilson Tang WH. Plasma Trimethylamine N-Oxide, a Gut Microbe-Generated Phosphatidylcholine Metabolite, Is Associated With Atherosclerotic Burden. *J. Am. Coll. Cardiol.* [Internet] J Am Coll Cardiol; 2016 [cited 2021 Sep 1]; 67: 2620–2628Available from: https://pubmed.ncbi.nlm.nih.gov/27256833/.

66. Aldana-Hernández P, Leonard KA, Zhao YY, Curtis JM, Field CJ, Jacobs RL. Dietary choline or trimethylamine N-oxide supplementation does not influence atherosclerosis development in Ldlr−/− and Apoe−/− male mice. *J. Nutr.* [Internet] J Nutr; 2020 [cited 2021 Sep 16]; 150: 249–255Available from: https://pubmed.ncbi.nlm.nih.gov/31529091/.

67. Xue J, Allaband C, Zhou D, Poulsen O, Martino C, Jiang L, Tripathi A, Elijah E, Dorrestein PC, Knight R, Zarrinpar A, Haddad GG. Influence of Intermittent Hypoxia/Hypercapnia on Atherosclerosis, Gut Microbiome, and Metabolome. *Front. Physiol.* [Internet] Frontiers Media SA; 2021 [cited 2021 Sep 20]; 12: 663950Available from: /pmc/articles/PMC8060652/.

68. Xue J, Zhou D, Poulsen O, Imamura T, Hsiao YH, Smith TH, Malhotra A, Dorrestein P,

Knight R, Haddad GG. Intermittent Hypoxia and Hypercapnia Accelerate Atherosclerosis, Partially via Trimethylamine-Oxide. *Am. J. Respir. Cell Mol. Biol.* [Internet] Am J Respir Cell Mol Biol; 2017 [cited 2022 Jul 12]; 57: 581–588Available from: https://pubmed.ncbi.nlm.nih.gov/28678519/.

69. Duttaroy AK. Role of Gut Microbiota and Their Metabolites on Atherosclerosis, Hypertension and Human Blood Platelet Function: A Review. *Nutrients* [Internet] Nutrients; 2021 [cited 2022 Jul 12]; 13: 1–17Available from: https://pubmed.ncbi.nlm.nih.gov/33401598/.

70. Bermudez-Brito M, Plaza-Díaz J, Muñoz-Quezada S, Gómez-Llorente C, Gil A. Probiotic mechanisms of action [Internet]. Ann. Nutr. Metab. Ann Nutr Metab; 2012 [cited 2021 Sep 18]. p. 160–174Available from: https://pubmed.ncbi.nlm.nih.gov/23037511/.

71. Sanchez-Rodriguez E, Egea-Zorrilla A, Plaza-Díaz J, Aragón-Vela J, Muñoz-Quezada S, Tercedor-Sánchez L, Abadia-Molina F. The gut microbiota and its implication in the development of atherosclerosis and related cardiovascular diseases [Internet]. Nutrients Nutrients; 2020 [cited 2021 Sep 18].Available from: https://pubmed.ncbi.nlm.nih.gov/32110880/.

72. Farrokhian A, Raygan F, Soltani A, Tajabadi-Ebrahimi M, Sharifi Esfahani M, Karami AA, Asemi Z. The Effects of Synbiotic Supplementation on Carotid Intima-Media Thickness, Biomarkers of Inflammation, and Oxidative Stress in People with Overweight, Diabetes, and Coronary Heart Disease: a Randomized, Double-Blind, Placebo-Controlled Trial. *Probiotics Antimicrob. Proteins* [Internet] Probiotics Antimicrob Proteins; 2019 [cited 2021 Sep 14]; 11: 133–142Available from:

https://pubmed.ncbi.nlm.nih.gov/29079990/.

73. Malik M, Suboc TM, Tyagi S, Salzman N, Wang J, Ying R, Tanner MJ, Kakarla M, Baker JE, Widlansky ME. Lactobacillus plantarum 299v supplementation improves vascular endothelial function and reduces inflammatory biomarkers in men with stable coronary artery disease. *Circ. Res.* [Internet] Circ Res; 2018 [cited 2021 Sep 14]; 123: 1091–1102Available from: https://pubmed.ncbi.nlm.nih.gov/30355158/.

74. Chan YK, El-Nezami H, Chen Y, Kinnunen K, Kirjavainen P V. Probiotic mixture VSL#3 reduce high fat diet induced vascular inflammation and atherosclerosis in ApoE−/− mice. *AMB Express* [Internet] AMB Express; 2016 [cited 2021 Sep 18]; 6Available from: https://pubmed.ncbi.nlm.nih.gov/27576894/.

75. Qiu L, Tao X, Xiong H, Yu J, Wei H. Lactobacillus plantarum ZDY04 exhibits a strain-specific property of lowering TMAO via the modulation of gut microbiota in mice. *Food Funct.* [Internet] Food Funct; 2018 [cited 2021 Sep 18]; 9: 4299–4309Available from: https://pubmed.ncbi.nlm.nih.gov/30039147/.

76. Rashid SK, Khodja NI, Auger C, Alhosin M, Boehm N, Oswald-Mammosser M, Schini-Kerth VB. Probiotics (VSL#3) prevent endothelial dysfunction in rats with portal hypertension: Role of the angiotensin system. *PLoS One* [Internet] Public Library of Science; 2014 [cited 2021 Sep 18]; 9: e97458Available from: https://journals.plos.org/plosone/article?id=10.1371/journal.pone.0097458.

77. Liu J, Li T, Wu H, Shi H, Bai J, Zhao W, Jiang D, Jiang X. Lactobacillus rhamnosus GG strain mitigated the development of obstructive sleep apnea-induced hypertension in a high salt diet via regulating TMAO level and CD4 + T cell induced-type I inflammation.

Biomed. Pharmacother. [Internet] Biomed Pharmacother; 2019 [cited 2022 Jul 12]; 112Available from: https://pubmed.ncbi.nlm.nih.gov/30784906/.

78. Xu H, Wang J, Cai J, Feng W, Wang Y, Liu Q, Cai L. Protective Effect of Lactobacillus rhamnosus GG and its Supernatant against Myocardial Dysfunction in Obese Mice Exposed to Intermittent Hypoxia is Associated with the Activation of Nrf2 Pathway. *Int. J. Biol. Sci.* [Internet] Int J Biol Sci; 2019 [cited 2022 Jul 12]; 15: 2471–2483Available from: https://pubmed.ncbi.nlm.nih.gov/31595164/.

79. Golbidi S, Badran M, Ayas N, Laher I. Cardiovascular consequences of sleep apnea [Internet]. Lung Lung; 2012 [cited 2020 Oct 7]. p. 113–132Available from: https://pubmed.ncbi.nlm.nih.gov/22048845/.

80. Koch CD, Gladwin MT, Freeman BA, Lundberg JO, Weitzberg E, Morris A. Enterosalivary nitrate metabolism and the microbiome: Intersection of microbial metabolism, nitric oxide and diet in cardiac and pulmonary vascular health. *Free Radic. Biol. Med.* [Internet] Free Radic Biol Med; 2017 [cited 2022 Jul 12]; 105: 48–67Available from: https://pubmed.ncbi.nlm.nih.gov/27989792/.

81. Wu BG, Sulaiman I, Wang J, Shen N, Clemente JC, Li Y, Laumbach RJ, Lu SE, Udasin I, Le-Hoang O, Perez A, Alimokhtari S, Black K, Plietz M, Twumasi A, Sanders H, Malecha P, Kapoor B, Scaglione BD, Wang A, Blazoski C, Weiden MD, Rapoport DM, Harrison D, Chitkara N, Vicente E, Marin JM, Sunderram J, Ayappa I, Segal LN. Severe Obstructive Sleep Apnea Is Associated with Alterations in the Nasal Microbiome and an Increase in Inflammation. *Am. J. Respir. Crit. Care Med.* [Internet] Am J Respir Crit Care Med; 2019 [cited 2022 Jul 12]; 199: 99–109Available from:

https://pubmed.ncbi.nlm.nih.gov/29969291/.

82. Dickson RP, Erb-Downward JR, Falkowski NR, Hunter EM, Ashley SL, Huffnagle GB. The Lung Microbiota of Healthy Mice Are Highly Variable, Cluster by Environment, and Reflect Variation in Baseline Lung Innate Immunity. *Am. J. Respir. Crit. Care Med.* [Internet] Am J Respir Crit Care Med; 2018 [cited 2022 Jul 12]; 198: 497–508Available from: https://pubmed.ncbi.nlm.nih.gov/29533677/.

Figures Legends:

Fig.1: **Alterations in fecal bacterial composition between IH and RA FMT with or without probiotic treatment.** Principal coordinate analysis plots ordinated using weighted UniFrac (**A**) and unweighted UniFrac (**B**) distances. Relative abundance of the five distinct ASVs found differentially abundant by ANCOM and ALDeX2 (**C**). FMT: fecal matter transplantation, IH: intermittent hypoxia, PRO: probiotic, RA: room air. Statistical analysis was done using two-way ANOVA followed by Tukey post-test •$p<0.05$ vs. IH-FMT, *$p < 0.05$ vs. IH-FMT-PRO, $^{\#}p < 0.05$ vs. RA-FMT, $^{\$}p < 0.05$ vs. RA-FMT-PRO. FMT: fecal matter transplantation, IH: intermittent hypoxia, PRO: probiotic, RA: room air, VEH: vehicle.

Fig. 2: FMT from IH-exposed mice elevates BP in naïve mice, and such BP changes are prevented by VSL3 probiotic treatment. Systolic blood pressure (SBP) (**A**), diastolic blood pressure (DBP) (**B**), mean blood pressure (MBP) (**C**). Values are displayed as mean ± S.D (n = 10) mice. Statistical analysis was done using two-way ANOVA followed by Tukey post-test *$p < 0.05$ vs. IH-FMT-PRO, $^{\#}p < 0.05$ vs. RA-FMT, $^{\$}p < 0.05$ vs. RA-FMT-PRO. FMT: fecal matter transplantation, IH: intermittent hypoxia, PRO: probiotic, RA: room air, VEH: vehicle

Fig. 3: FMT from IH-exposed mice impairs coronary arteries function in naïve mice and VSL3 probiotic administration prevents such effects. Cumulative concentration response curve of U46619 (**A**), acetylcholine (ACh) (**B**), and sodium nitroprusside (SNP) (**C**). Values are displayed as mean ± S.D (n = 9 -10) mice. Statistical analysis was done using two-way ANOVA followed by Tukey post-test *$p < 0.05$ vs. IH-FMT-PRO, $^{\#}p < 0.05$ vs. RA-FMT, $^{\$}p < 0.05$ vs. RA-FMT-PRO. FMT: fecal matter transplantation, IH: intermittent hypoxia, PRO: probiotic, RA: room air, VEH: vehicle

Fig. 4: FMT from IH exposed mice increases TMAO plasma levels and decreases acetate plasma levels, and VSL3 probiotics restore TMAO but not acetate plasma concentrations. Plasma TMAO levels (**A**), Plasma acetate concentrations (**B**). Values are displayed as mean ± S.D (n = 5) mice. Statistical analysis was done using two-way ANOVA followed by Tukey post-test *$p < 0.05$ vs. IH-FMT-PRO, $^{\#}p < 0.05$ vs. RA-FMT, $^{\$}p < 0.05$ vs. RA-FMT-PRO. FMT: fecal matter transplantation, IH: intermittent hypoxia, PRO: probiotic, RA: room air, TMAO: trimethylamine N-oxide, VEH: vehicle

Fig. 5: VSL3 probiotic administration does not lower elevated BP or prevent coronary artery dysfunction in mice exposed to IH. Mean arterial blood pressure (MBP) (**A**), Cumulative concentration response curve of U46619 (**B**), acetylcholine (ACh) (**C**), and sodium nitroprusside (SNP) (**D**). Values are displayed as mean ± S.D (n = 8-10) mice. Statistical analysis was done using two-way ANOVA followed by Tukey post-test *$p < 0.05$ vs. RA. IH: intermittent hypoxia, PRO: probiotic, RA: room air

Fig. S1: Relative abundance of taxa at greater than 5% at phylum (**A**) and family (**B**) levels. All taxa with less than 5% relative abundance were grouped into the" Other" category. FMT: fecal matter transplantation, IH: intermittent hypoxia, RA: room air

Fig. S2: EMPress plot depicting the phylogenetic tree of all features detected by 16S rRNA amplicon sequencing with concentric circles describing the following feature metadata from the innermost layer out: phylum, relative abundance within treatment group, W-score produced by ANCOM, Benjamani Hochberg-corrected p value of ALDEx2 generalized linear model and features significantly differing identified by ALDEx2 or ALDEx2 and ANCOM. FMT: fecal matter transfer, IH: intermittent hypoxia, PRO: probiotic, RA: room air

Fig. S3: Hierarchical cluster analysis of the 50 consistently detected ASVs in the gut microbiota. FMT: fecal matter transfer, IH: intermittent hypoxia, ASV: amplicon sequence variant, PRO: probiotic, RA: room air

Fig. S4: FMT from IH-exposed mice impairs aortic function in naïve mice and VSL3 probiotic administration prevents such effects. Cumulative concentration response curve of U46619 (**A**), acetylcholine (ACh) (**B**), and sodium nitroprusside (SNP) (**C**). Values are displayed as mean ± S.D (n = 9 -10) mice. Statistical analysis was done using two-way ANOVA followed by Tukey post-test *$p < 0.05$ vs. IH-FMT-PRO, $^{\#}p < 0.05$ vs. RA-FMT, $^{\$}p < 0.05$ vs. RA-FMT-PRO. FMT: fecal matter transplantation, IH: intermittent hypoxia, PRO: probiotic, RA: room air, VEH: vehicle

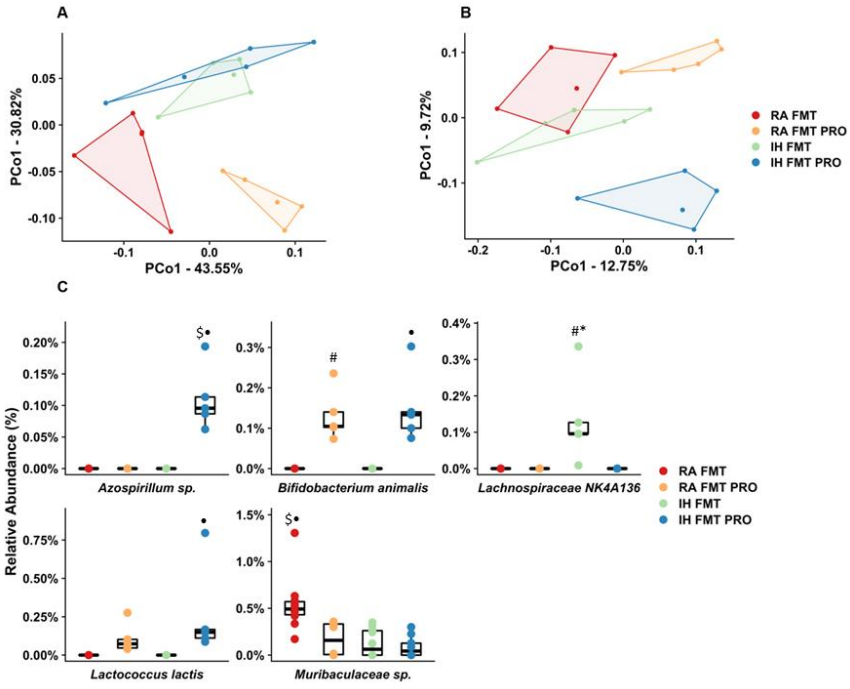
A
PCo1 - 30.82%
PCo1 - 43.55%
B
PCo1 - 9.72%
PCo1 - 12.75%
RA FMT
RA FMT PRO
IH FMT
IH FMT PRO
C
Relative Abundance (%)
Azospirillum sp.
Bifidobacterium animalis
Lachnospiraceae NK4A136
Lactococcus lactis
Muribaculaceae sp.
$
#
#*

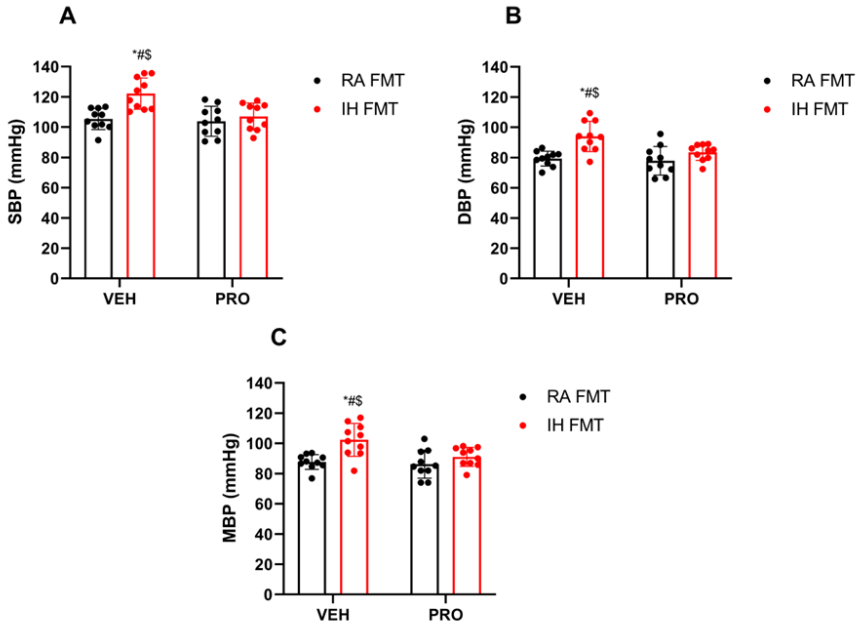
A
SBP (mmHg)
140
120
100
80
60
40
20
0
*#$
VEH
PRO
RA FMT
IH FMT
B
DBP (mmHg)
140
120
100
80
60
40
20
0
*#$
VEH
PRO
RA FMT
IH FMT
C
MBP (mmHg)
140
120
100
80
60
40
20
0
*#$
VEH
PRO
RA FMT
IH FMT

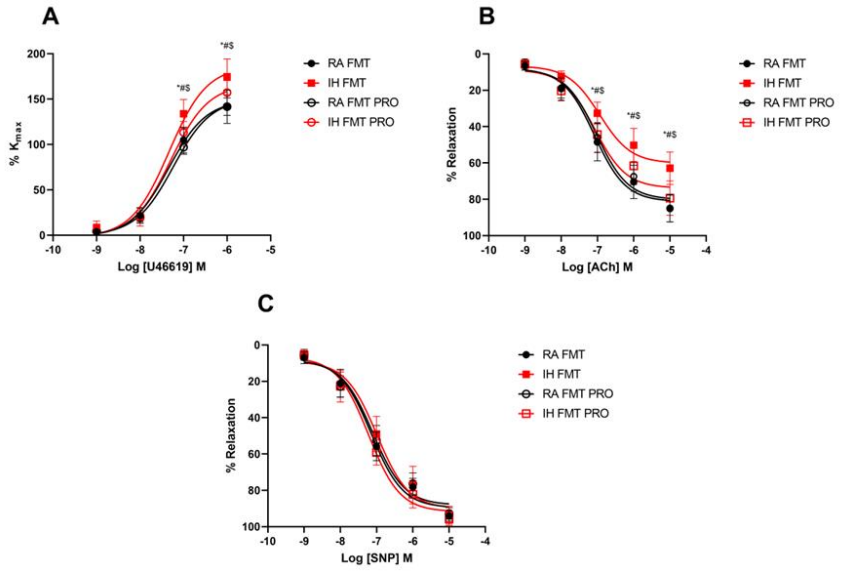
A
% K_{max}
Log [U46619] M
RA FMT
IH FMT
RA FMT PRO
IH FMT PRO
B
% Relaxation
Log [ACh] M
C
% Relaxation
Log [SNP] M

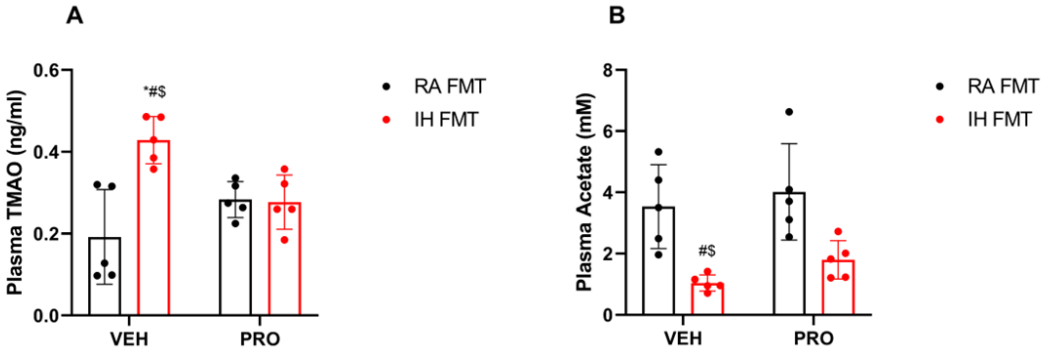
A
Plasma TMAO (ng/ml)
0.6
0.4
0.2
0.0
*#$
VEH
PRO
RA FMT
IH FMT
B
Plasma Acetate (mM)
8
6
4
2
0
#$
VEH
PRO
RA FMT
IH FMT

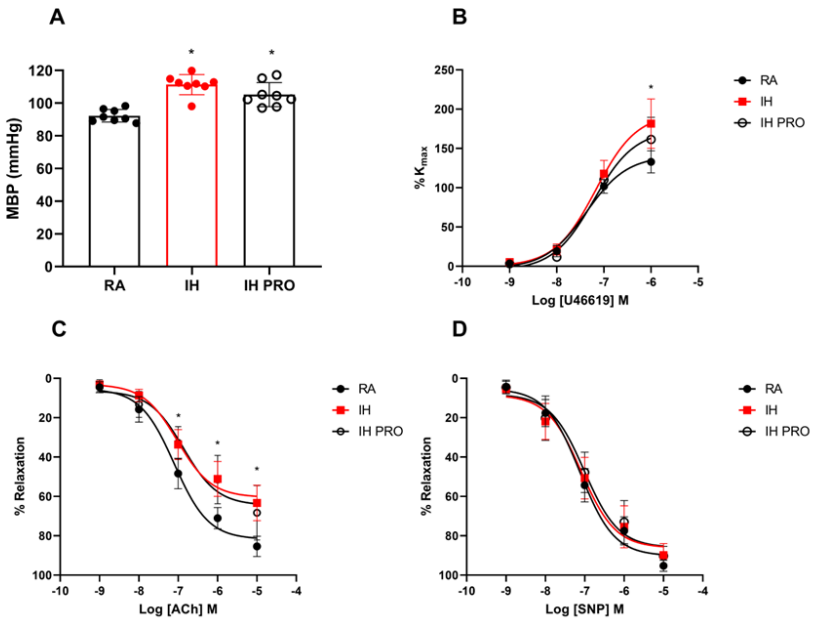
A
MBP (mmHg)
120
100
80
60
40
20
0
RA
IH
IH PRO
*
*
B
% Kmax
250
200
150
100
50
0
-10
-9
-8
-7
-6
-5
Log [U46619] M
RA
IH
IH PRO
*
C
% Relaxation
0
20
40
60
80
100
-10
-9
-8
-7
-6
-5
-4
Log [ACh] M
RA
IH
IH PRO
*
*
*
D
% Relaxation
0
20
40
60
80
100
-10
-9
-8
-7
-6
-5
-4
Log [SNP] M
RA
IH
IH PRO

Supplementary materials

Table S1: Significant relative abundance taxa in in gut microbiome composition in naïve mice subjected to FMT from mice exposed to RA and IH and treated with VSL3

Taxon	Relative Abundance (Mean ± SD)				ANCOM	ALDEx2	
	RA FMT	RA FMT PRO	IH FMT	IH FMT PRO	W score	glm.ep	glm.eBH
d__Bacteria; p__Firmicutes; c__Bacilli; o__Erysipelotrichales; f__Erysipelotrichaceae; g__Dubosiella; s__uncultured_bacterium	3.75% ± 1.23%	0.44% ± 0.27%	1.77% ± 0.89%	15.05% ± 5.65%		6.96E-09	4.05E-06
d__Bacteria; p__Bacteroidota; c__Bacteroidia; o__Bacteroidales; f__Muribaculaceae; g__Muribaculaceae; s__uncultured_Bacteroidales	0.59% ± 0.17%	0.91% ± 0.26%	0.69% ± 0.05%	0.32% ± 0.02%		8.86E-08	2.11E-05
d__Bacteria; p__Bacteroidota; c__Bacteroidia; o__Bacteroidales; f__Muribaculaceae; g__Muribaculaceae; s__uncultured_bacterium	0.08% ± 0.03%	0.15% ± 0.04%	0.41% ± 0.04%	0.26% ± 0.07%		8.94E-08	2.24E-05
d__Bacteria; p__Bacteroidota; c__Bacteroidia; o__Bacteroidales; f__Muribaculaceae; g__Muribaculaceae; s__uncultured_Bacteroidales	0.72% ± 0.29%	0.19% ± 0.05%	0.07% ± 0.04%	0.16% ± 0.07%		5.72E-07	1.13E-04
d__Bacteria; p__Bacteroidota; c__Bacteroidia; o__Bacteroidales; f__Muribaculaceae; g__Muribaculaceae; s__uncultured_bacterium	0.41% ± 0.16%	0.33% ± 0.02%	0.00% ± 0.00%	0.00% ± 0.00%	1700	1.25E-06	1.67E-04
d__Bacteria; p__Firmicutes; c__Bacilli; o__Lactobacillales; f__Streptococcaceae; g__Lactococcus; s__Lactococcus_lactis	0.00% ± 0.00%	0.11% ± 0.10%	0.00% ± 0.00%	0.26% ± 0.30%	1591	7.52E-06	5.09E-04
d__Bacteria; p__Proteobacteria; c__Gammaproteobacteria; o__Burkholderiales; f__Sutterellaceae; g__Parasutterella; s__uncultured_organism	0.25% ± 0.13%	1.00% ± 0.17%	0.11% ± 0.10%	0.16% ± 0.04%		4.14E-06	5.30E-04
d__Bacteria; p__Bacteroidota; c__Bacteroidia; o__Bacteroidales; f__Muribaculaceae; g__Muribaculaceae; s__uncultured_organism	0.67% ± 0.36%	0.01% ± 0.01%	0.26% ± 0.09%	0.17% ± 0.09%	1623	7.93E-06	6.13E-04
d__Bacteria; p__Bacteroidota; c__Bacteroidia; o__Bacteroidales; f__Muribaculaceae; g__Muribaculaceae; s__uncultured_bacterium	19.29% ± 4.36%	17.86% ± 4.95%	8.05% ± 1.08%	6.76% ± 3.20%		4.97E-06	6.58E-04
d__Bacteria; p__Actinobacteriota; c__Actinobacteria; o__Bifidobacteriales; f__Bifidobacteriaceae; g__Bifidobacterium; s__Bifidobacterium_animalis	0.00% ± 0.00%	0.13% ± 0.06%	0.00% ± 0.00%	0.15% ± 0.09%	1631	2.05E-05	1.09E-03
d__Bacteria; p__Bacteroidota; c__Bacteroidia; o__Bacteroidales; f__Muribaculaceae; g__Muribaculaceae; s__uncultured_bacterium	0.35% ± 0.11%	0.30% ± 0.05%	0.11% ± 0.03%	0.36% ± 0.13%		2.28E-05	1.83E-03
d__Bacteria; p__Firmicutes; c__Bacilli;	0.65% ±	0.04% ±	0.16% ±	2.40% ±		5.17E-05	2.93E-03

o__Erysipelotrichales; f__Erysipelotrichaceae; g__Dubosiella; s__uncultured_bacterium	0.22%	0.06%	0.08%	0.89%			
d__Bacteria; p__Bacteroidota; c__Bacteroidia; o__Bacteroidales; f__Muribaculaceae; g__Muribaculaceae; s__uncultured_bacterium	0.42% ± 0.13%	0.12% ± 0.02%	0.30% ± 0.10%	0.41% ± 0.21%		5.08E-05	3.52E-03
d__Bacteria; p__Bacteroidota; c__Bacteroidia; o__Bacteroidales; f__Rikenellaceae; g__Alistipes; s__uncultured_bacterium	0.24% ± 0.14%	0.66% ± 0.19%	0.19% ± 0.09%	0.55% ± 0.10%		6.14E-05	4.14E-03
d__Bacteria; p__Firmicutes; c__Bacilli; o__Lactobacillales; f__Lactobacillaceae; g__Lactobacillus	5.89% ± 2.04%	1.99% ± 0.41%	10.49% ± 8.26%	2.20% ± 0.45%		6.79E-05	4.72E-03
d__Bacteria; p__Actinobacteriota; c__Coriobacteriia; o__Coriobacteriales; f__Atopobiaceae; g__Coriobacteriaceae_UCG-002; s__uncultured_bacterium	0.13% ± 0.09%	0.21% ± 0.15%	0.07% ± 0.02%	0.69% ± 0.31%		1.22E-04	6.89E-03
d__Bacteria; p__Bacteroidota; c__Bacteroidia; o__Bacteroidales; f__Muribaculaceae; g__Muribaculaceae; s__uncultured_Bacteroidales	0.45% ± 0.27%	0.83% ± 0.22%	0.05% ± 0.05%	1.92% ± 0.89%		2.62E-04	9.45E-03
d__Bacteria; p__Actinobacteriota; c__Coriobacteriia; o__Coriobacteriales; f__Eggerthellaceae; g__Enterorhabdus	0.10% ± 0.05%	0.05% ± 0.02%	0.17% ± 0.04%	0.19% ± 0.02%		2.33E-04	9.79E-03
d__Bacteria; p__Proteobacteria; c__Alphaproteobacteria; o__Rhodospirillales; f__uncultured; g__uncultured; s__Azospirillum_sp.	0.00% ± 0.00%	0.00% ± 0.00%	0.00% ± 0.00%	0.11% ± 0.05%	1577	5.48E-04	1.21E-02
d__Bacteria; p__Firmicutes; c__Clostridia; o__Lachnospirales; f__Lachnospiraceae; g__Lachnospiraceae_NK4A136_group	0.00% ± 0.00%	0.00% ± 0.00%	0.13% ± 0.12%	0.00% ± 0.00%	1557	5.36E-04	1.27E-02
d__Bacteria; p__Proteobacteria; c__Gammaproteobacteria; o__Burkholderiales; f__Sutterellaceae; g__Parasutterella; s__uncultured_bacterium	0.70% ± 0.22%	0.43% ± 0.09%	0.97% ± 0.18%	1.15% ± 0.22%		3.64E-04	1.47E-02
d__Bacteria; p__Firmicutes; c__Bacilli; o__RF39; f__RF39; g__RF39	0.01% ± 0.00%	0.00% ± 0.00%	0.02% ± 0.01%	0.05% ± 0.05%		7.27E-04	1.51E-02
d__Bacteria; p__Firmicutes; c__Clostridia; o__Clostridia_UCG-014; f__Clostridia_UCG-014; g__Clostridia_UCG-014	0.00% ± 0.01%	0.01% ± 0.02%	0.17% ± 0.08%	0.03% ± 0.02%		5.52E-04	1.60E-02
d__Bacteria; p__Firmicutes; c__Clostridia; o__Clostridia_UCG-014; f__Clostridia_UCG-014; g__Clostridia_UCG-014	0.01% ± 0.02%	0.19% ± 0.13%	0.18% ± 0.07%	0.02% ± 0.03%		6.09E-04	1.67E-02
d__Bacteria; p__Bacteroidota; c__Bacteroidia; o__Bacteroidales; f__Muribaculaceae; g__Muribaculaceae; s__uncultured_bacterium	0.21% ± 0.13%	0.08% ± 0.02%	0.08% ± 0.02%	0.03% ± 0.02%		5.29E-04	1.73E-02
d__Bacteria; p__Bacteroidota; c__Bacteroidia; o__Bacteroidales; f__Muribaculaceae; g__Muribaculaceae; s__uncultured_bacterium	1.20% ± 0.28%	2.24% ± 0.93%	2.72% ± 0.96%	3.39% ± 0.56%		5.48E-04	1.98E-02
d__Bacteria; p__Firmicutes; c__Clostridia;	0.00% ±	0.01% ±	0.04% ±	0.03% ±		1.28E-03	2.05E-02

o__Clostridiales; f__Clostridiaceae; g__Clostridium_sensu_stricto_1	0.00%	0.01%	0.01%	0.01%			
d__Bacteria; p__Firmicutes; c__Clostridia; o__Oscillospirales; f__Oscillospiraceae; g__uncultured; s__uncultured_Clostridiales	0.19% ± 0.10%	0.24% ± 0.11%	0.33% ± 0.09%	0.73% ± 0.30%		7.03E-04	2.27E-02
d__Bacteria; p__Firmicutes; c__Bacilli; o__Erysipelotrichales; f__Erysipelotrichaceae; g__Ileibacterium; s__Ileibacterium_valens	28.57% ± 5.19%	28.77% ± 13.01%	39.26% ± 7.85%	16.60% ± 5.86%		6.82E-04	2.35E-02
d__Bacteria; p__Firmicutes; c__Clostridia; o__Oscillospirales; f__Oscillospiraceae; g__Colidextribacter	0.06% ± 0.03%	0.00% ± 0.00%	0.03% ± 0.04%	0.05% ± 0.03%		1.64E-03	2.66E-02
d__Bacteria; p__Bacteroidota; c__Bacteroidia; o__Bacteroidales; f__Rikenellaceae; g__Alistipes; s__uncultured_bacterium	0.04% ± 0.02%	0.22% ± 0.14%	0.43% ± 0.33%	0.32% ± 0.16%		8.68E-04	2.68E-02
d__Bacteria; p__Firmicutes; c__Clostridia; o__Clostridia_UCG-014; f__Clostridia_UCG-014; g__Clostridia_UCG-014	0.00% ± 0.00%	0.03% ± 0.02%	0.15% ± 0.05%	0.01% ± 0.01%		1.70E-03	2.99E-02
d__Bacteria; p__Bacteroidota; c__Bacteroidia; o__Bacteroidales; f__Muribaculaceae; g__Muribaculaceae; s__uncultured_bacterium	1.61% ± 0.66%	1.11% ± 0.10%	2.83% ± 1.25%	3.75% ± 0.78%		1.06E-03	3.14E-02
d__Bacteria; p__Firmicutes; c__Bacilli; o__Erysipelotrichales; f__Erysipelatoclostridiaceae; g__Erysipelatoclostridium; s__unidentified	0.09% ± 0.06%	0.07% ± 0.02%	0.00% ± 0.01%	0.00% ± 0.00%		2.08E-03	3.31E-02
d__Bacteria; p__Actinobacteriota; c__Coriobacteriia; o__Coriobacteriales; f__Eggerthellaceae; g__Enterorhabdus; s__uncultured_bacterium	0.05% ± 0.03%	0.15% ± 0.01%	0.04% ± 0.03%	0.05% ± 0.01%		1.45E-03	3.44E-02
d__Bacteria; p__Firmicutes; c__Clostridia; o__Lachnospirales; f__Lachnospiraceae	0.00% ± 0.00%	0.00% ± 0.00%	0.00% ± 0.00%	0.03% ± 0.01%		2.58E-03	3.78E-02
d__Bacteria; p__Firmicutes; c__Clostridia; o__Lachnospirales; f__Lachnospiraceae	0.10% ± 0.08%	0.00% ± 0.00%	0.03% ± 0.03%	0.00% ± 0.00%		3.20E-03	3.80E-02
d__Bacteria; p__Firmicutes; c__Clostridia; o__Oscillospirales; f__UCG-010; g__UCG-010; s__unidentified	0.04% ± 0.02%	0.09% ± 0.03%	0.01% ± 0.01%	0.00% ± 0.00%		3.93E-03	3.84E-02
d__Bacteria; p__Firmicutes; c__Bacilli; o__Erysipelotrichales; f__Erysipelotrichaceae; g__Faecalibaculum; s__uncultured_bacterium	0.14% ± 0.04%	0.62% ± 0.36%	0.30% ± 0.15%	0.14% ± 0.01%		1.60E-03	3.91E-02
d__Bacteria; p__Firmicutes; c__Bacilli; o__Lactobacillales; f__Streptococcaceae; g__Streptococcus; s__Streptococcus_danieliae	0.00% ± 0.00%	0.00% ± 0.00%	0.03% ± 0.01%	0.00% ± 0.00%		2.39E-03	4.16E-02
d__Bacteria; p__Firmicutes; c__Clostridia; o__Oscillospirales; f__[Eubacterium]_coprostanoligenes_group; g__[Eubacterium]_coprostanoligenes_group; s__uncultured_bacterium	0.00% ± 0.00%	0.00% ± 0.00%	0.06% ± 0.05%	0.01% ± 0.01%		3.15E-03	4.34E-02
d__Bacteria; p__Firmicutes; c__Clostridia;	0.04% ±	0.33% ±	0.05% ±	0.00% ±		2.80E-03	4.66E-02

o__Oscillospirales; f__Ruminococcaceae; g__Incertae_Sedis; s__uncultured_bacterium	0.05%	0.12%	0.06%	0.00%			
d__Bacteria; p__Firmicutes; c__Clostridia; o__Peptococcales; f__Peptococcaceae; g__uncultured; s__unidentified	0.04% ± 0.05%	0.00% ± 0.00%	0.03% ± 0.02%	0.07% ± 0.03%		5.07E-03	4.76E-02
d__Bacteria; p__Actinobacteriota; c__Coriobacteriia; o__Coriobacteriales; f__Eggerthellaceae; g__Gordonibacter; s__uncultured_bacterium	0.13% ± 0.08%	0.19% ± 0.04%	0.08% ± 0.05%	0.05% ± 0.01%		2.54E-03	4.91E-02

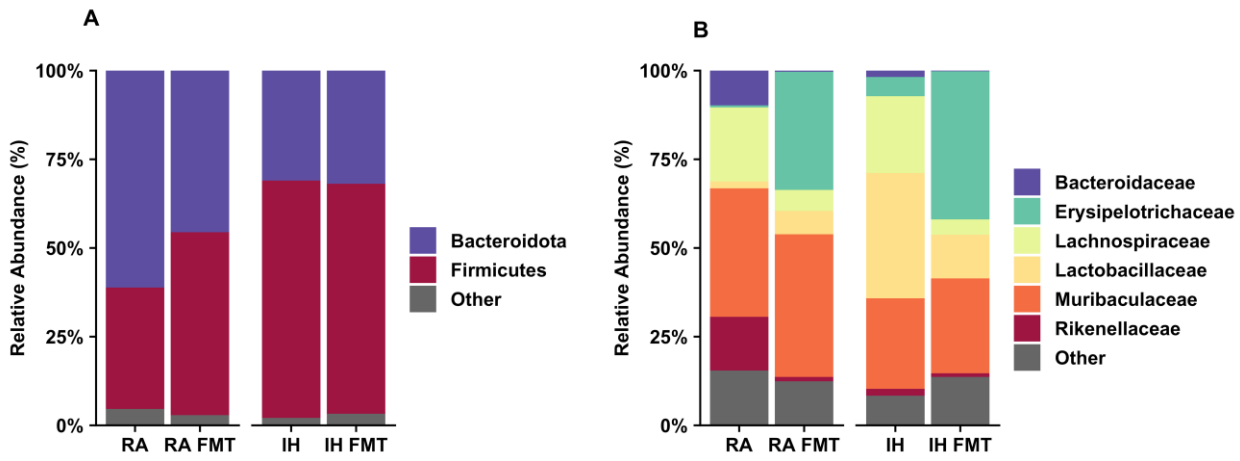
A
100%
75%
50%
25%
0%
Relative Abundance (%)
RA
RA FMT
IH
IH FMT
Bacteroidota
Firmicutes
Other
B
100%
75%
50%
25%
0%
Relative Abundance (%)
RA
RA FMT
IH
IH FMT
Bacteroidaceae
Erysipelotrichaceae
Lachnospiraceae
Lactobacillaceae
Muribaculaceae
Rikenellaceae
Other

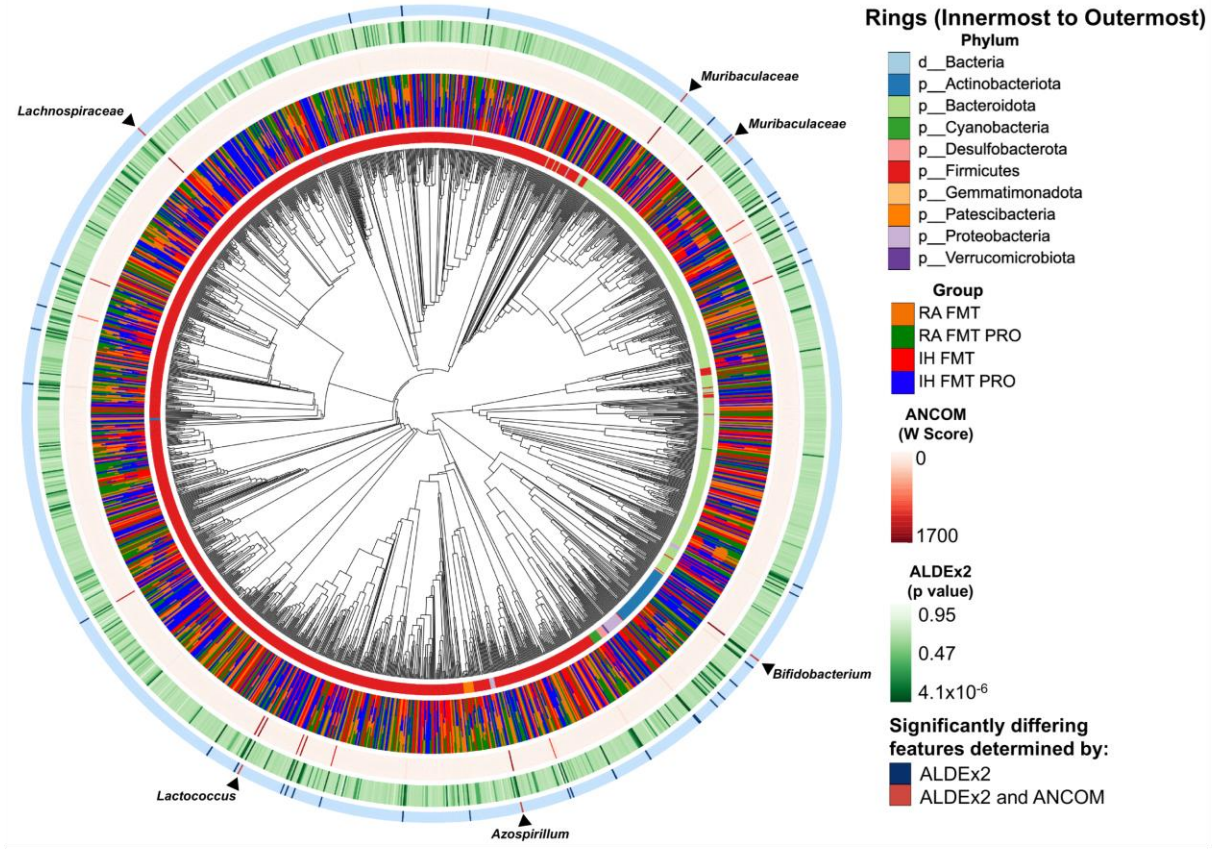
Lachnospiraceae
Muribaculaceae
Muribaculaceae
Bifidobacterium
Lactococcus
Azospirillum
Rings (Innermost to Outermost)
Phylum
d__Bacteria
p__Actinobacteriota
p__Bacteroidota
p__Cyanobacteria
p__Desulfobacterota
p__Firmicutes
p__Gemmatimonadota
p__Patescibacteria
p__Proteobacteria
p__Verrucomicrobiota
Group
RA FMT
RA FMT PRO
IH FMT
IH FMT PRO
ANCOM
(W Score)
0
1700
ALDEx2
(p value)
0.95
0.47
4.1x10-6
Significantly differing
features determined by:
ALDEx2
ALDEx2 and ANCOM

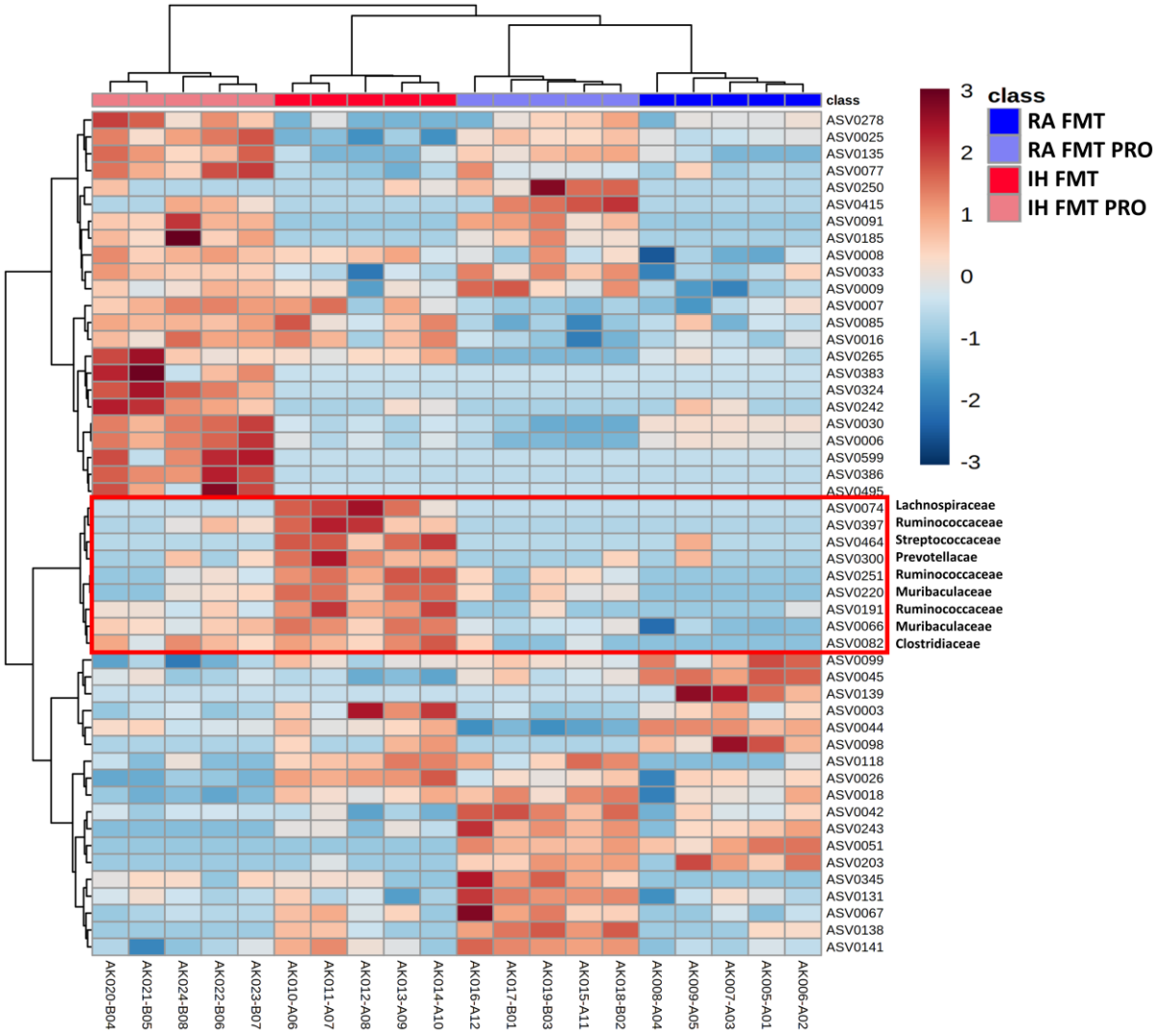
class
ASV0278
ASV0025
ASV0135
ASV0077
ASV0250
ASV0415
ASV0091
ASV0185
ASV0008
ASV0033
ASV0009
ASV0007
ASV0085
ASV0016
ASV0265
ASV0383
ASV0324
ASV0242
ASV0030
ASV0006
ASV0599
ASV0386
ASV0495
ASV0074
ASV0397
ASV0464
ASV0300
ASV0251
ASV0220
ASV0191
ASV0066
ASV0082
ASV0099
ASV0045
ASV0139
ASV0003
ASV0044
ASV0098
ASV0118
ASV0026
ASV0018
ASV0042
ASV0243
ASV0051
ASV0203
ASV0345
ASV0131
ASV0067
ASV0138
ASV0141
Lachnospiraceae
Ruminococcaceae
Streptococcaceae
Prevotellacae
Ruminococcaceae
Muribaculaceae
Ruminococcaceae
Muribaculaceae
Clostridiaceae
AK020-B04
AK021-B05
AK024-B08
AK022-B06
AK023-B07
AK010-A06
AK011-A07
AK012-A08
AK013-A09
AK014-A10
AK016-A12
AK017-B01
AK019-B03
AK015-A11
AK018-B02
AK008-A04
AK009-A05
AK007-A03
AK005-A01
AK006-A02
3
2
1
0
-1
-2
-3
class
RA FMT
RA FMT PRO
IH FMT
IH FMT PRO

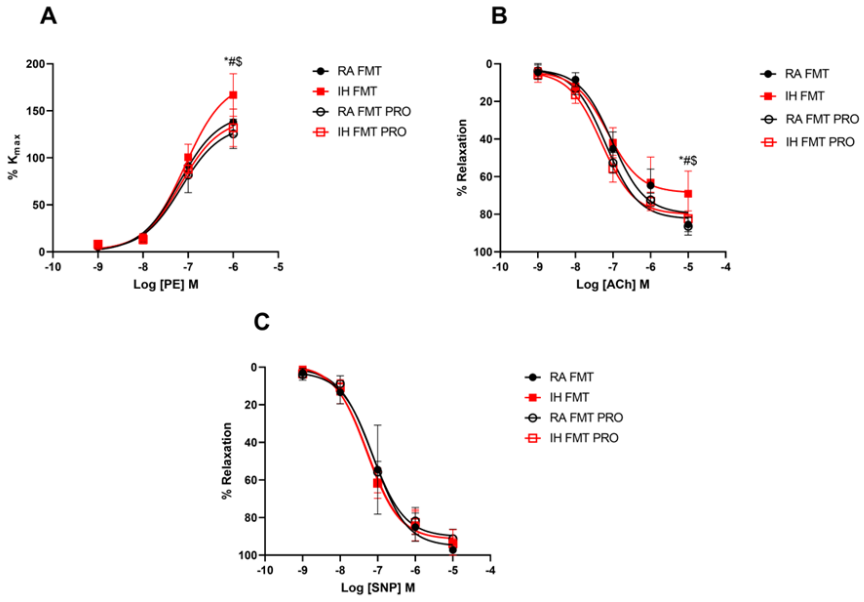
A
B
C
RA FMT
IH FMT
RA FMT PRO
IH FMT PRO
% Kmax
Log [PE] M
% Relaxation
Log [ACh] M
Log [SNP] M
*#$